AN ABSTRACT OF THE THESIS OF

ARTHUR JOHN MALIK for the DOCTOR OF PHILOSOPHY
(Name) (Degree)

in General Science presented on 2 July 1973
(Major) (Date)

Title: A STUDY OF THE EXCITED STATES OF ^{30}P USING THE REACTION ^{29}Si(p, γ)^{30}P

Abstract approved: Redacted for privacy

The ^{29}Si(p, γ)^{30}P reaction has been used to study the excited states in ^{30}P populated by the γ-decay of the resonance states at E_p = 2040, 2084, 2125, 2234, and 2410 KeV. The branching ratios of these resonance states to the bound states in ^{30}P were determined using $^{29}SiO_2$ targets on gold backings and recording the γ-ray spectra with a high resolution Ge(Li) detector. A new level at 5.58 MeV is proposed. This level is excited by the γ-decay of the 2040 KeV resonance. The level at 4343 KeV, populated by the γ-decay of the 2410 KeV resonance, has not previously been studied in any (p, γ) resonance experiments.

Precision γ-ray energy measurements at E_p = 2040 and 2125 KeV resonances yield the energies of the bound states of ^{30}P with errors ranging between 0.5 to 2 KeV. Nineteen levels were excited

and their excitation energies (in KeV) determined as follows:

677.4 ± 0.5; 709.2 ± 0.5; 1454.6 ± 0.5; 1973.7 ± 0.7; 2539.2 ± 1.0; 2724.0 ± 0.5; 2839.9 ± 1.0; 2938.2 ± 1.0; 3020.1 ± 0.5; 3836.2 ± 1.2; 4183.2 ± 1.2; 4422.0 ± 2.0; 4736.7 ± 1.0; 4938.5 ± 1.0; 5206.6 ± 2.0; 5507.1 ± 1.0; 5576.9 ± 2.0; 5702.3 ± 1.0.

The Q-value of the reaction $^{29}Si(p, \gamma)^{30}P$ was determined to be $Q = 5591.5 \pm 3$ KeV.

The Doppler-shift attenuation method (DSAM) was used to measure, or place limits on, lifetimes of several states in ^{30}P with excitation energies $E_x < 5.8$ MeV. The attenuated Doppler-shifts were obtained by detecting the γ-rays at $\theta = 0°$, $90°$, and $120°$ at $E_p = 2125$ KeV and at $\theta = 0°$ and $120°$ at $E_p = 2040$ and 2410 KeV resonances. These resonances were chosen because their dominant modes of decay are to states in the $E_x = 2538$ to 5710 KeV range, for which only limited prior data exist. The measured lifetimes (in fsec.) are as follows:

2539 KeV level (262 ± 10), 2724 KeV level (190 ± 25), 2839 KeV level (2200 ± 800), 3020 KeV level (< 21), 3836 KeV level (52 ± 8), 4183 KeV level (< 20), 4343 KeV level (220 ± 25), 4422 KeV level (62 ± 8), 4736 KeV level (90 ± 14), 4939 KeV level (< 15), 5206 KeV level (30 ± 15), 5507 KeV level (< 10), 5577 KeV level (< 21), and 5702 KeV level (< 21).

The lifetimes of the levels at E_x = 4736, 5206, 5506, 5577, and 5702 KeV have not previously been measured.

Finally, the results obtained in this work are compared to the earlier measurements, and nuclear model calculations.

A Study of the Excited States of ^{30}P Using the Reaction $^{29}Si(p,\gamma)^{30}P$

by

Arthur John Malik

A THESIS

submitted to

Oregon State University

in partial fulfillment of
the requirements for the
degree of

Doctor of Philosophy

June 1974

APPROVED:

Redacted for privacy

Associate Professor of Physics

in charge of major

Redacted for privacy

Chairman of Department of General Science

Redacted for privacy

Dean of Graduate School

Date thesis is presented 2 July 1973

Typed by Illa W. Atwood for Arthur John Malik

ACKNOWLEDGMENT

I wish to express my gratitude to Dr. L. Wayne Swenson for proposing this problem, for many discussions concerning all aspects of this work, and for the continuous help and encouragement needed to complete it.

The O.S.U. computer center has advanced a computer grant without which the data analysis would not have been possible.

The Society of Sigma Xi provided financial support for the purchase of the target.

Thanks are also due to the Nucelar Physics group at the University of Oregon, especially Dr. D. K. McDaniels, who not only loaned their accelerator facilities, but also assisted with some data taking.

The assistance of Mr. Keith King of the General Science Department in reducing the size of the γ-ray spectra charts is highly appreciated.

Finally, I would like to thank my wife, Vimla, for her moral support and her help in proofreading this manuscript.

TABLE OF CONTENTS

LIST OF FIGURES

LIST OF TABLES

A STUDY OF THE EXCITED STATES OF ^{30}P USING THE REACTION $^{29}Si(p,\gamma)^{30}P$

I. INTRODUCTION

The discovery of the fine structure in alpha-spectra from naturally radioactive substances first led to the conception of nuclear energy levels in analogy with Bohr's successful electronic energy level scheme to explain atomic spectra. Similarly, emission of β-rays was observed to lead to the formation of daughter nuclei in various excited states. These excited states are subsequently observed to decay by the emission of γ-rays of discrete energies corresponding to the excitation energy of the daughter nucleus. With the discovery and development of high energy accelerators, it has become possible to produce nuclides in a great variety of excited states by nuclear scattering and reactions. A great deal of spectroscopic information on the energy levels of nuclei (especially light nuclei) has now been accumulated from such studies.

The aim of the research in low energy nuclear physics is to measure accurately the properties of the atomic nucleus, e.g. mass, electric and magnetic moments, charge and matter distributions, transition rates, and such properties of individual levels as spin, parity, excitation energies, etc. A theoretical formulation of nuclear structure must, in the final analysis, be capable of predicting all the

various measured parameters. Unfortunately, the nucleus consists of a relatively small number (less than 250) of strongly interacting particles. Small in the sense that there are not sufficient particles to make plausible the use of statistical or many-body methods to describe the bulk properties of the system. Unlike the atom it is also not obvious that there is any dominant central interaction such that the residual interaction between nucleons can be treated as a small correction to the independent motion of the nucleons in a central field. Furthermore, the nucleon-nucleon interaction, which is attractive to within a small distance of approximately 2 fm. but becomes strongly repulsive within a separation distance of 0.4 fm. has velocity dependent, spin dependent, and non-central terms. These terms are of a sufficiently complicated form that the theoretical techniques necessary for the description of such a system and the capacity (and speed) of computing systems have only recently advanced to the point where realistic calculations are feasible.

In the absence of a completely satisfactory detailed theory of nuclear structure, attempts have been made to correlate nuclear data in terms of rough pictures or models of the nucleus. A model is a mathematical construct which supposedly contains all the features essential to explain some body of physical phenomena. At the present time, there exists a collection of models of the nucleus each of which is capable of organizing or explaining a limited portion of the

presently available experimental data. None of these models is, however, by itself a complete description of nuclear behavior.

Information on nuclear structure, and thereby on the correlations brought about by nuclear interactions within the nucleus, can often be extracted from the study of electromagnetic interactions in nuclei. Gamma-ray transition probabilities (lifetimes) between two nuclear states depend on the multipolarity, the energy of the γ-rays, and the wavefunctions of the nuclear states involved in the transition. Gamma-ray transition probabilities are proportional to the reduced matrix elements, $\langle \psi_f \| \theta_\ell \| \psi_i \rangle$, where ψ_f and ψ_i are nuclear wavefunctions of the final and initial states and θ_ℓ is the electromagnetic operator of order ℓ. The experimental determination of these matrix elements is important because they are a direct and sensitive test of nuclear wavefunctions without any detailed dependence on nuclear forces or reaction mechanisms. Thus one of the most stringent tests of a nuclear model is its ability to reproduce the experimentally observed radiative lifetimes. A less sensitive test of a particular model is its ability to reproduce the experimentally observed spectra of energy levels with given spin and parity for a set of nuclei. It is a less sensitive test because the energies are stationary with respect to small variations in the model wavefunctions.

The aim of the measurements described in this work is to

contribute to the understanding of the structure of ^{30}P states by making precise measurements of the γ-ray energies, branching ratios, and lifetimes of several states of ^{30}P populated in the γ-decay of resonant states of ^{30}P.

II. BACKGROUND

2.1. The Radiative Proton Capture Reactions

The study of gamma-rays emitted during charged particle bombardment has become increasingly important in recent years as an approach to the spectroscopy of nuclear energy levels. Most comprehensive studies of the gamma-radiation from nuclear reactions are being made possible by recent advances in instrumentation. Of the various particle accelerators the Van de Graaff electrostatic generator has come into the greatest favor for such work because of the accurate and continuous control of beam energy, small energy beam spread, small beam spot dimensions, a beam that can be steady or pulsed, and low machine background. The advent of the Ge(Li) gamma-ray detector has made the investigation of radiative particle capture reactions an even more powerful tool in nuclear spectroscopy than it has been up to now. The most obvious advantage of the high resolution Ge(Li) detector over the conventional NaI detector is, besides the resolution of close multiplets, the possibility of more precise determinations of gamma-ray transition energies and thus of level energies.

There are many different ways by which energy can be given to a nucleus in order to excite its virtual states, for example, ^{30}P nucleus can be excited to its virtual levels by the following reactions:

$^{27}Al(\alpha,n)^{30}P$; $^{28}Si(\alpha,d)^{30}P$; $^{29}Si(p,\gamma)^{30}P$; $^{29}Si(d,n)^{30}P$; $^{30}Si(p,n)^{30}P$; $^{31}P(p,d)^{30}P$; $^{32}S(d,\alpha)^{30}P$; etc. For the present investigation, $^{29}Si(p,\gamma)^{30}P$ capture-gamma reaction was chosen. There are a number of advantages of using this reaction. The first advantage is that it is possible to populate virtual states at high excitation energies. The Q-value of the reaction $^{29}Si(p,\gamma)^{30}P$, that is, the difference in the rest mass energies of the ingoing and outgoing particles, is 5597 ± 3 KeV (1). Thus it is possible to populate excited states of ^{30}P at energies above 5597 KeV relative to the ground state energy whenever the incident proton has sufficient energy to penetrate the Coulomb barrier. In this region, few channels are open for particle emission which would compete strongly with the capture-gamma reaction. At low bombarding energies, it is possible to excite well-isolated virtual states (resonant states). Isolated resonances have the important advantage that the reaction mechanism is well understood. Therefore, one advantage of the radiative-capture reaction is that information can be obtained on the properties of many excited states from the study of a single resonance spectrum.

The second advantage of the (p,γ) reaction is that every resonance has its characteristic decay scheme, such that close lying members of a doublet or triplet will be excited with different intensities at different resonances; in a favorable case only one member will participate in the decay with measurable intensity.

The third advantage of (p, γ) reaction is the relatively simple kinematics involved. There are only two particles involved in the ingoing case, the incident particle and the target nucleus, and only one particle in the outgoing case, the recoiling nucleus in an excited state. Conservation of both the energy and the momentum give the following result:

$$E_x = Q + E_{cm},$$

where E_x is the energy of excitation of the recoiling compound nucleus and E_{cm} is the incident particle center-of-mass energy i. e.

$$E_{cm} = \frac{m}{M} E_p,$$

where m is the mass of incident proton and M is the mass of the compound nucleus, E_p is the energy of the incident proton in the laboratory frame of reference. Thus the energy of the resonant state selectively excited in the capture-gamma reaction is determined by the measurement of only one quantity, the incident proton energy, when the reaction-Q is known.

2.2. Competing Reactions

In addition to gamma-decay a resonant state can decay by particle emission, such as neutrons, protons, alphas or any other nuclear fragments when the energy of the excited state is greater

than the binding energy of the particle. In a proton-capture reaction the resonant excited state can always decay by proton emission since the probability of formation through a particular channel is equal to the probability of decay through that channel. A condition for successful observation of radiative proton-capture (capture of protons by the nucleus with subsequent emission of gamma-rays) is that the binding energy of the neutrons, alpha-particles, and other nuclear fragments be higher than that of the proton. When this condition is not satisfied, a virtual excited state can decay by neutron or alpha-particle emission in competition with protons and gamma-rays. Since the electromagnetic forces are much weaker than the nuclear forces, electromagnetic radiation usually competes unfavorably with particle emission. The study of the capture reaction can be considerably hindered by this competition.

In the case of ^{30}P, the neutron-proton binding energy difference is

$$E_b(n) - E_b(p) = 5731 \text{ KeV},$$

so only for proton energies greater than 5731 KeV (2) is the emission of neutrons energetically possible. Since the alpha-particle-proton binding energy difference is 4818 KeV (2), the $^{29}Si(p, \alpha)^{26}Al$ reaction is also not possible. At proton energies used in this work, the $^{29}Si(p, p')^{29}Si$ reaction can populate the first (1273 KeV) and the second (2032 KeV) levels in ^{29}Si. The 1273-KeV level decays

entirely to the ground state while the 2032-KeV level goes 95% to the ground state, so $^{29}Si(p,p')^{29}Si$ reaction can produce only two gamma-lines, one at 1273-KeV and the other at 2032-KeV, in the gamma-ray spectrum of $^{29}Si(p,\gamma)^{30}P$ reaction. $^{30}P(\beta^+)^{30}Si$ produces a 2230-KeV line, which appears as a contaminant in the $^{29}Si(p,\gamma)^{30}P$ gamma-ray spectrum.

2.3. Contaminant Gamma-rays

Studies of capture gamma-rays induced by protons or alphas are frequently complicated by the presence of contaminants either in the target material itself or on the backing. In the case of proton induced reactions, the most common contaminant is ^{19}F which gives rise, through the reaction $^{19}F(p,\alpha\gamma)^{16}O$, to 6129.3-KeV gamma-rays. The energy of this gamma-ray is well-known (3) and was used as a high-energy calibration point. Other important contaminants for protons are nitrogen which produces 4.43-MeV gamma-rays from the reaction $^{15}N(p,\alpha\gamma)^{12}C$, sodium which gives rise to a very great number of resonances for the (p,γ) and $(p,\alpha\gamma)$ reactions. The most commonly observed gamma-rays are 439-KeV, 1633-KeV, 1368-KeV which are produced by $^{23}Na(p,p')^{23}Na$; $^{23}Na(p,\alpha\gamma)^{20}Ne$; and $^{23}Na(p,\gamma)^{24}Mg$ reactions respectively, and carbon which produces capture-gamma-rays at a number of resonances from the $^{12}C(p,\gamma)^{13}N$ and $^{13}C(p,\gamma)^{14}N$ reactions. The presence of carbon isotopes usually

comes from carbon build-up on the targets during bombardment. This can be reduced considerably by providing a very cold surface as close as possible to the target. In the present work the carbon contamination was essentially eliminated by the use of a liquid nitrogen cold trap in the beam transport system. Great care has to be exercised in preparing and handling the targets. Sweaty finger prints, for example, can make excellent thin sodium targets.

Some room-background gamma-ray peaks, with well-known energies, appear in the gamma-ray spectra. The gamma-rays of energy 1460.75-KeV (4) and 2614.47-KeV (5), for example, are due to the natural occurrence of ^{40}K in concrete and ^{232}Th in lead respectively. These two gamma-ray peaks provided excellent calibration points.

Contribution to the gamma-ray spectrum of the reaction $^{29}Si(p,\gamma)^{30}P$ from the other isotopes of Si such as ^{28}Si and ^{30}Si was essentially eliminated by the use of targets enriched in ^{29}Si.

2.4. Doppler Shift Attenuation Method (DSAM) for Lifetime Measurements

The Doppler shift attenuation method compares the nuclear lifetime with the slowing-down time of the recoiling excited nucleus in the material through which it is passing. If the lifetime is long compared to the slowing down time, most of the excited nuclei decay

at rest and if the lifetime is very short, compared to the slowing down time, the nuclei decay in flight before slowing down. In the former case, there is little change in the gamma-ray energy due to Doppler effect, while in the latter case one observes the maximum Doppler shift. For an intermediate case the observed energy shift is a function of the lifetime, and it is in this region that the DSAM is most useful.

A typical experimental arrangement for measuring the Doppler shift is shown in Figure 1. The proton beam from an accelerator is

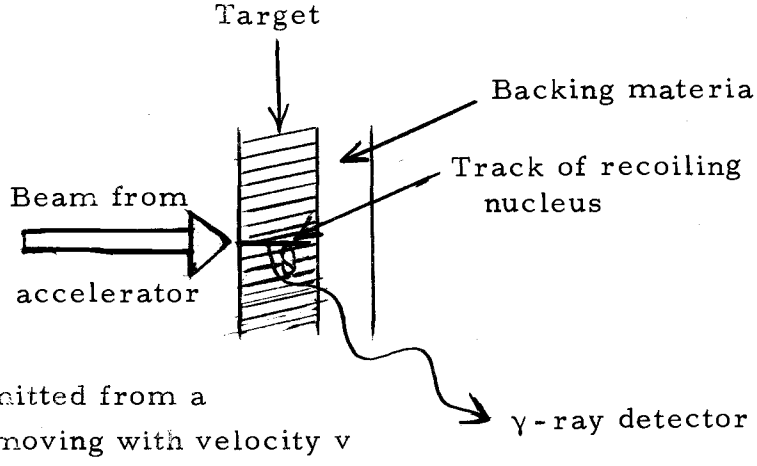

Figure 1. Experimental Arrangement for Measuring the Doppler Shifts

incident from the left onto the target of some element. Nuclear reactions induced in this target by the proton beam produce recoiling excited nuclei, moving with a velocity

$$v = \frac{\left(2E_p m_p\right)^{\frac{1}{2}}}{M},$$

where M is the mass of the recoiling nucleus, m_p is the mass of incident proton, and E_p is the kinetic energy of the incident proton, which then rapidly slow down in the target deposit or the backing material. The backing is usually chosen to be a high Z material; a low energy ion beam will then, because of the higher coulomb barrier of the backing material, produce few nuclear reactions in the backing, resulting in low background. Targets of this kind are usually made by evaporating the target material onto some backing material (Tantalum, Gold, Carbon).

For a source (the recoiling excited nucleus) moving towards a stationary observer (the gamma detector), the frequency change $\Delta\nu$ seen by the stationary observer is given by:

$$\frac{\Delta\nu}{\nu_0} = \frac{v}{c} \quad \text{for } \frac{v}{c} << 1,$$

where ν_0 = frequency from stationary source, v = source velocity, and c = velocity of light. Since for a photon $E = h\nu$, then

$$\frac{\Delta E}{E_0} = \frac{v}{c} \quad \text{or} \quad \Delta E = \frac{E_0 v}{c}.$$

If the angle between the direction of the source and the observer is θ, then

$$\Delta E_\gamma(\theta) = E_0 \frac{v}{c} \cos\theta.$$

So the energy of the gamma-radiation emitted from nuclei formed at

$t = 0$ and moving thereafter with a velocity $v(t)$ is given by:

$$E_\gamma = E_0 \left(1 + \frac{v(t)}{c} \cos\theta\right) \text{ for } \frac{v(t)}{c} << 1 \qquad (1)$$

If the recoiling nuclei are slowed down and eventually stopped in a material, the observed shift is smaller than the maximum shift

$$E = E_0 \left(1 + \frac{v(0)}{c} \cos\theta\right) \qquad (2)$$

Use of eq (1) and exponential decay law enables one to deduce that the attenuation factor, defined as the ratio of the observed shift and the maximum expected shift, is given by:

$$F(\tau) = \frac{\Delta E_{observed}}{\Delta E_{expected}} = \frac{(E_\gamma - E_0)_{observed}}{(E_\gamma - E_0)_{expected}} = \frac{\frac{v(t)}{c}\cos\theta}{\frac{v(0)}{c}\cos\theta}$$

$$= \left\langle \frac{v(t)}{v(0)} \right\rangle = \frac{\int_0^\infty \frac{v(t)}{v(0)} e^{-\frac{t}{\tau}} dt}{\int_0^\infty e^{-\frac{t}{\tau}} dt} = \frac{1}{\tau}\int_0^\infty \frac{v(t)}{v(0)} e^{-\frac{t}{\tau}} dt$$

where τ is the mean lifetime of the decaying nucleus. The above equation is valid only if all the recoil ions travel in the same direction. However, the nuclear collisions cause the beam of recoiling nuclei to diverge and this produces a further attenuation effect. An expression for the attenuation factor, based on the work of Blaugrund (6) for large angle scattering due to nuclear collisions and on the stopping power theory of heavy ions developed by Lindhard et al. (7),

is given by:

$$F(\tau) = \frac{1}{\tau} \int_0^\infty \frac{v(t)}{v(0)} \; e^{-\frac{t}{\tau}} \; \overline{\cos\phi(t)} \; dt, \qquad (3)$$

where $\overline{\cos\phi(t)}$ is the average of the cosine of the angles through which the recoiling nuclei have been scattered at time t. The lifetime of the gamma-emitting state is determined by comparing the experimentally determined $F(\tau)$, given by

$$F(\tau) = \frac{\Delta E_{observed}}{\Delta E_{expected}} = \frac{E_\gamma(\theta_1) - E_\gamma(\theta_2)}{\frac{v(0)}{c}(\cos\theta_1 - \cos\theta_2)}$$

with the numerical solutions of eq (3). Since the lifetimes of the resonance levels generally are immeasurably short (less than 1 fs.) this technique can be used to determine the lifetime of states populated directly from the resonance level.

A somewhat more complicated situation arises when the level of interest is populated from a state with a measurable lifetime. Then $F(\tau)$ is given by:

$$F(\tau) = \frac{\tau_1 F_1 - \tau_2 F_2}{\tau_1 - \tau_2},$$

where the subscripts 1 and 2 refer to the parent and daughter levels respectively. The lifetime of the daughter level can be determined if the mean lifetime of the parent level is known.

A still more complicated situation occurs when the level under

investigation is populated partly by feeding from the resonance level (assumed to have negligible lifetime) and partly by a level of finite lifetime. Then

$$F(\tau) = (1 - r)F_2 + r\left[\frac{\tau_1 F_1 - \tau_2 F_2}{\tau_1 - \tau_2}\right],$$

where r = fraction fed via state of finite lifetime, and subscripts 1, 2 are as defined above for the level of finite lifetime and the level of interest. The Doppler shift attenuation method, as described by Devon et al. (8), Litherland et al. (9), Warburton et al. (10), has proved to be very effective for the determination of lifetimes of nuclear energy levels in the range from 10^{-11} to 10^{-15} sec., especially since large Ge(Li) detectors with good resolution and reasonable efficiency have become available. Ideal reactions for Doppler-shift measurements are radiative resonant capture (p, γ) and (α, γ) reactions because they can produce excited nuclei travelling in a well defined direction (without the use of coincidence method) at 0.5 percent to 1 percent of the velocity of light. However, the usefulness of the (p, γ) reactions for studying isolated resonances and Doppler shifts is limited to light nuclei ($A \leq 50$) because of rapid increase of the coulomb barrier and density of states with increasing A. The large coulomb barrier relative to the proton energy results in low yields and high density of states implies many closely spaced resonances which are difficult to study selectively. Also, in radiative

capture reactions the bombarding energies are low (because of the reasons noted above and also to be below the threshold for particle emission from the compound nucleus) and the recoil velocities are then low also. On the other hand, in using particle-in particle-out reactions which provide high recoil velocities, coincidence measurements must be made in order to establish the recoil direction. The counting rates obtainable are consequently low, due to the low efficiency of the Ge(Li) detector. One important difficulty in the study of the DSAM at low initial velocities is that the slowing down process is more complex than in the case of high initial velocities in which the electronic stopping power dominates the slowing down process. At low initial velocity, the electronic slowing down is rapidly replaced by nuclear slowing down. The nuclear collisions, besides slowing down the recoiling ions also change their directions. This complicates the analysis of the nuclear lifetime data (6) as expressed by eq. (3).

Recently, the DSAM has come under some criticism. Several experimental studies have shown that the nuclear lifetimes measured by the DSAM are subject to systematic errors in analysis which are considerably larger than the experimental errors. A dependence of the results of DSA measurements on the stopping material has been known for some time. Currie et al. (11) studied the line shapes of the ground state transition of the first excited state in ^{30}Si for

different backing materials (Mg, Ni, Sn, Y, Au). They found a variation of 1.45, in which the lifetime was strongly correlated with the observed attenuation factor, i.e., with the stopping power of the slowing medium. Their conclusion was that the major uncertainty in DSA measurements stems from the inadequacy of the present stopping power theory (LSS Theory) and that the root mean square error from this source will be nearly 15 percent in a typical measurement. The same kind of trend has since been pointed out from independent experiments (12, 13, 14).

There are some sources of systematic error in the description of the slowing down process according to Lindhard theory (7). First, there are oscillations of the experimental electronic stopping cross-sections as a function of the atomic number of the recoil nuclei about the Lindhard values (15). These oscillations are damped out at high velocities (16) and there is evidence that they are also damped out if heavy stopping atoms are used (17). Another uncertainty comes from the fact that the nuclear part of the slowing down process has not yet been determined experimentally; thus its energy dependence may differ from the theory especially at low velocities. Moreover, it is not clear, if it is correct to treat the electronic and nuclear parts of the stopping power independently in the region where both are comparable in magnitude. A detailed experimental study of these complex problems is highly desirable.

2.5. Review of ^{30}P Levels

The level structure of the odd-odd ^{30}P nucleus has been the object of a number of investigations during the past few years. Most of the information about the energies, spins, and parities of the excited states has been obtained by means of the $^{32}S(d, \alpha)^{30}P$ (18) reaction, the $^{28}Si(He^3, p\gamma)^{30}P$ (19) reaction, and the $^{29}Si(p, \gamma)^{30}P$ (1, 20-29) reaction, while the lifetime information for the levels in ^{30}P has come from the $^{29}Si(p, \gamma)^{30}P$ (29, 31-34), and the $^{27}Al(\alpha, n\gamma)^{30}P$ (35-38) reactions.

Endt and Paris (18), using the reaction $^{32}S(d, \alpha)^{30}P$, located the energies of 30 excited states in ^{30}P up to 5.8-MeV excitation energy.

Angular correlation measurements have been performed by Vermette et al. (19) using the reaction $^{28}Si(^3He, p\gamma)^{30}P$. Information on spins, mixing ratios, and branching ratios were obtained for 16 levels in ^{30}P below 5-MeV excitation energy. This paper also gives theoretical values of the lifetimes of the levels up to 2939 KeV which were obtained by applying, on a harmonic oscillator basis, the shell model mixtures of two $1d_{\frac{1}{2}} - 2s_{\frac{1}{2}}$ nucleons outside a ^{28}Si core which had been calculated by Glaudemans, Wiechers, and Brussaard (39).

Resonances in the $^{29}Si(p, \gamma)^{30}P$ reaction for proton energies below 2 MeV have been studied by a number of investigators. Van

der Leun and Endt (20); Baart et al. (21); and Broud et al. (22) investigated the proton resonances below 1 MeV. Decay schemes and branching ratios of the resonances at E_p = 326, 414, 693, 729, 920, and 960 KeV were studied and the spins, parities, and isobaric spins of several bound states in ^{30}P were established using the results of single gamma-ray spectra, coincidence, and angular distribution measurements. Moor (23) studied the proton resonances in the energy region E_p = 1.1 to 1.8 MeV; Val'ter et al. (24) and Ejiri et al. (25) covered the proton energy region 1.1 to 1.4 KeV and L'vov et al. (26) extended the energy region to 2.5 MeV. Phelps et al. (27) and Bergstrom-Rohlin (28) determined the gamma-decay of the proton resonances in the proton energy range 1.46 to 1.86 MeV and 1.9 to 2.16 MeV respectively. In all the above mentioned studies, the NaI(Tℓ) scintillation counter was used for gamma-ray measurements. Using a Ge(Li) detector, Harris and Hyder (1) and Hyder et al. (29) reinvestigated the gamma-decay schemes of some 24 resonances in the proton energy region between 0.3 to 1.8 MeV. Several previously unreported transitions were found and decay schemes of several resonances revised considerably. Recently, Din and Davis (30) have studied the gamma-ray decay schemes of 14 resonances in the energy range E_p = 0.90 to 2.12 MeV using high resolution Ge(Li) detectors. They reported decay to the bound levels at 3.84, 4.74, 4.94, 5.21, 5.51, and 5.70 MeV in ^{30}P. These levels have

previously been excited by the $^{32}S(d,\alpha)^{30}P$ (18) reaction, but not by any $^{29}Si(p,\gamma)^{30}P$ resonances. The excitation energies are summarized in Figure 2, together with the branching ratio, spin, and parity information.

The lifetimes of levels in ^{30}P have been determined using the Doppler-shift attenuation method, by a number of investigators. Using the reaction $^{29}Si(p,\gamma)^{30}P$, Graves and McDaniels (31), Harris et al. (29), Lachaine and Hird (32), Bini et al. (33), and Luukko et al. (34) have determined the lifetimes of several of the bound levels in ^{30}P below 5 MeV excitation energy. Recently, the $^{27}Al(\alpha,n\gamma)^{30}P$ reaction has been used in DSA measurements by Sharpey-Schafer et al. (35, 36), Kennedy et al. (37), and Pixley and Poletti (38). Recently, Hanson et al. (40) have measured the lifetimes of the 1453 and 1974-MeV levels in ^{30}P via the reaction $^{27}Al(\alpha,n\gamma)^{30}P$ and recoil distance method. These measurements should provide a useful check on those obtained from the $^{29}Si(p,\gamma)^{30}P$ reaction and also give some information on levels not populated in this reaction, e.g. 4296, 4343 MeV levels in ^{30}P.

The mean lifetimes of several levels, found by different investigators, are in disagreement often by considerable amounts. Also, there have been no measurements of the lifetimes of the 4.74, 5.21, 5.51, 5.58, and 5.70 MeV levels in ^{30}P. It is the aim of this investigation to determine the lifetimes of these levels and attempt to make

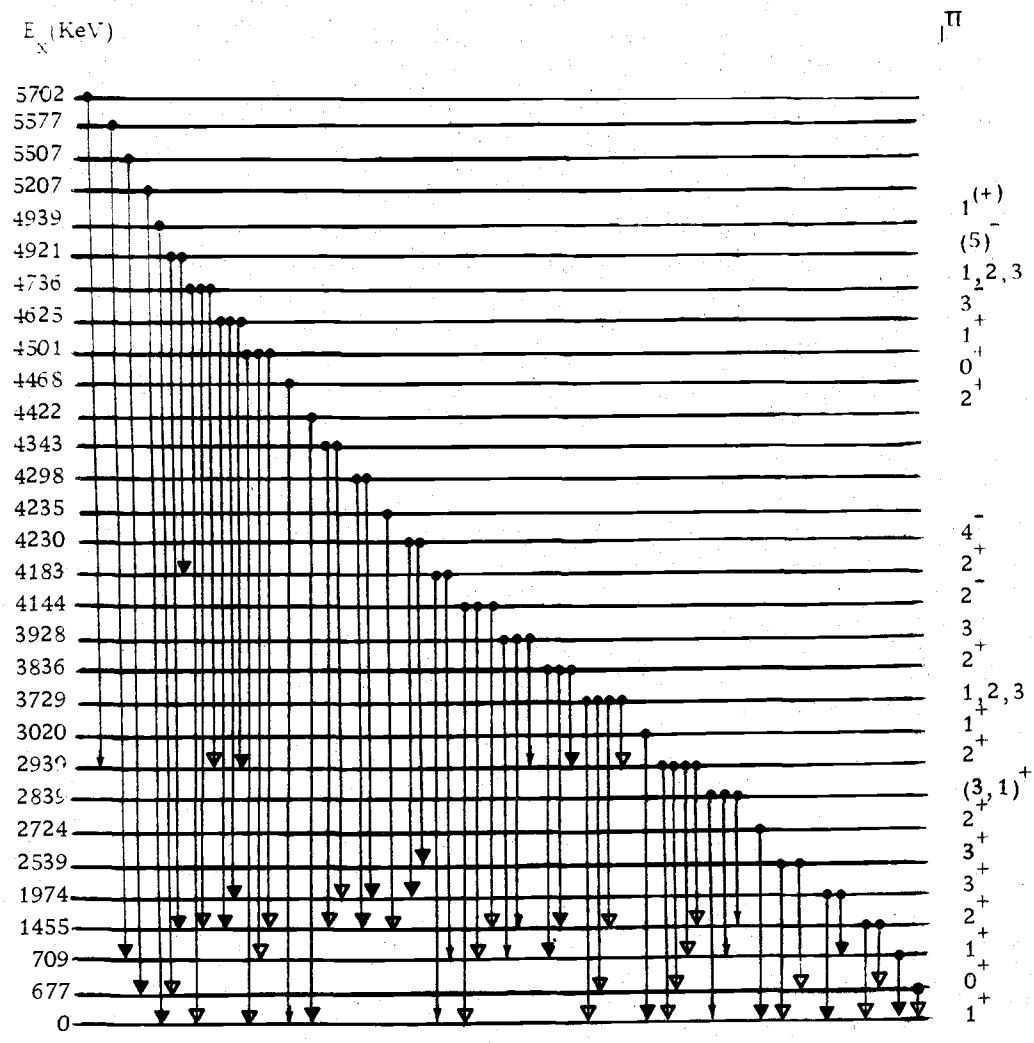

Figure 2. Energy Level Diagram of ^{30}P. The data used are taken from the present work and the references (19, 29, 30, 35, 36).

more precise measurements of the lifetimes of the other levels in ^{30}P excited in the gamma-decay of the 2.040, 2.125, and 2.410-MeV resonances.

2.6. Model Calculations

In recent years several models, of increasing complexity and extension, have been proposed for nuclei in the second half of the 2s - 1d shell. The success of the strong-coupling collective model (Nilsson model) in explaining the nuclear properties of the lower half of the 2s - 1d shell prompted similar calculations in the upper half of this shell. Baart, Green and Willmott (21) investigated the applicability of Nilsson model to ^{30}P and concluded that this model is inadequate to explain the observed levels of ^{30}P. Detailed calculations of Picard and Pinho (41) using a rotational Nilsson model with a Soper two-body force led to a satisfactory prediction of only the first two excited states. Wasielewski and Malik (42), and Ascuitto, Bell and Davidson (43) have investigated ^{30}P using a Nilsson model with Coriolis coupling between the rotational bands and a two-body interaction between the odd proton and odd neutron. They were successful in explaining the observed energy spectrum up to 4 MeV. Although the model can account for most of the transition rates, there are a few significant discrepancies for the transition rates involving states above 2 MeV. It seems that the model does not provide an adequate

description for nuclear states much above 2 MeV in these nuclei. Experimental studies indicate that the deformation of the nuclei in the 2s - 1d shell increases up to A = 22 - 25 and decreases thereafter and that the nuclear shape changes rather abruptly at A = 28 from prolate to oblate. Thus, the level structures of nuclei with A = 30 - 35 do not exhibit characteristic rotational features to the extent found, for example, in A = 20 - 25. Thankappan and Pandya (44) applied a weak-coupling model to ^{31}P and achieved better agreement with experimental results than they did using a strong coupling model. A calculation by Bouten et al. (45) using intermediate coupling SU_3 approach in a systematic study of the 2s - 1d nuclei was only partially successful in describing the low-lying states of ^{30}P and ^{34}Cl.

Recently, a more sophisticated vibrational unified model has been proposed by Singh et al. (46). This model is a modified version of the intermediate-coupling unified model, in which the anharmonic character of the core nucleus (^{32}S) used is taken into account. In addition pairing effects are also considered by coupling quasiparticle states to anharmonic vibrations of the core nucleus. This model gives good predictions of many properties of ^{30}P.

Glaudemans et al. (47) made shell model calculations for ^{30}P assuming an inert ^{28}Si core and two-particle interactions for the outer nucleons in the $2s_{1/2}$ and $1d_{3/2}$ shells. Although a number of level energies and spins were successfully explained, several of

the observed levels could not be reproduced by means of this truncated shell-model picture.

A substantial agreement with experiment was later realized when Wildenthal et al. (48) and Glaudemans et al. (49) made calculations in a vector space which includes basis states containing active $1d_{5/2}$, $2s_{1/2}$, and $1d_{3/2}$ sub-shell nucleons. These treatments of the shell-model resulted in excellent agreement between experimental spectroscopic data and the data predicted by the above model wavefunctions.

The energy levels predicted by the unified vibrational model of Singh et al. (46), recent shell-model calculations, and the recent experimental results are presented in Table 1.

Table 1. Experimental, Shell Model, and Intermediate Coupling Model Information Concerning the Excitation Energies and Transition Rates in ^{30}P. Data taken from Singh et al. (46).

$E_i \rightarrow E_f$ (MeV)	$J_i, T_i \rightarrow J_f, T_f$	Experiment				Intermediate-coupling model	Shell model
		Ref. a	Ref. b	Ref. c	Ref. d		
B(E2) rates in ^{30}P (in Weisskopf units)							
0.71 → 0	1,0 → 1,0	1.8 or 2.9			0.68 ± 0.13	0.5	0.7
1.45 → 0	2,0 → 1,0	0.10	0.08		0.34 $^{+0.19}_{-0.13}$	2.7	1.1
1.97 → 0	3,0 → 1,0	0.18	0.31		0.9 $^{+0.3}_{-0.2}$	0.05	0.5
1.97 → 0.71	3,0 → 1,0	2.5			12.5 ± 3.0	6.7	0.0
2.54 → 0	3,0 → 1,0	15	4.0		5.9 ± 0.6	5.4	0.0
2.54 → 0.71	3,0 → 1,0					0.2	1.3
2.72 → 0	2,0 → 1,0	9.2		6.0 ± 0.8	5.0 $^{+0.4}_{-1.0}$	4.5	0.0
2.84 → 0	3,0 → 1,0	0.048				1.5	
2.84 → 0.71	3,0 → 1,0	0.46				0.8	
2.84 → 1.45	3,0 → 2,0					2.6	
2.94 → 0	2,1 → 1,0	0.019 or 2.4			0.008 ± 0.013 or 0.92 ± 0.3	0	0.1
2.94 → 0.68	2,1 → 0,1	21		11.4 ± 1.4	8.2 ± 1.4	7.2	1.2
2.94 → 0.71	2,1 → 1,0					≈0	0.0
2.94 → 1.45	2,1 → 2,0				< 0.4	≈0	0.7
B(M1) rates in ^{30}P (in 10^{-2} Weisskopf units)							
0.68 → 0	0,1 → 1,0	65		63 $^{+9}_{-7}$		38	2.6
0.71 → 0	1,0 → 1,0	0.32 or 0.18		0.15 ± 0.02 or 0.008 ± 0.003		0.03	0.1
1.45 → 0	2,0 → 1,0	0.093	0.13	0.32 $^{+0.11}_{-0.08}$		0.16	0.0
1.45 → 0.71	2,0 → 1,0	0.057		0.10 $^{+0.04}_{-0.03}$		0.22	0.2
1.97 → 1.45	3,0 → 2,0	0.31				8.6	0.0
2.72 → 0	2,0 → 1,0	0.16		0.09 ± 0.06		0.02	0.0
2.84 → 1.45	3,0 → 2,0	0.092		0.34 ± 0.06		8.5	
2.94 → 0	2,1 → 1,0	0.56 or 0.12		0.22 ± 0.09 or 0.05 → 0.03		0.28	4.0
2.94 → 0.71	2,1 → 1,0	0.68		0.27 ± 0.04		0.09	9.8
2.94 → 1.45	2,1 → 2,0	11		4.3 ± 0.7		8.1	73

III. EXPERIMENTAL PROCEDURE

3. 1. Equipment

The proton beam was produced by the University of Oregon 4-MeV Van de Graaff accelerator. The beam is bent through an angle of 45° and deflected into the main experimental area by a homogeneous field analyzing magnet. The main experimental area is separated from the accelerator and the analyzing magnet by a 24-in. concrete wall. The beam is defined 76-in. before the magnet entrance by a water cooled focussing ring and 65-in. after the magnet exit by adjustable water-cooled vertical slits. Fine focussing of the beam is accomplished by quadrupole doublets located before the focussing ring and after the exit slits. Water-cooled collimators are positioned in the beam tube before an in-line cold trap at a distance of 15- and 32-in. from the target. The in-line liquid nitrogen trap located 10-in. in front of the target helps considerably in reducing background due to build-up of contaminants during bombardment. The target area is shielded on the top and all sides by 16-in. thick walls of solid concrete blocks to reduce background radiation due to scattered neutrons and gamma-rays. The machine energy is regulated by currents from the slits fed back to adjustable corona points to maintain a balanced current on the high and the low energy sides

of the slits. It is possible to maintain the machine stable over long periods of time.

The targets used in this experiment were 10 - 12 KeV thick SiO_2, enriched in ^{29}Si and deposited on 0.01-in. thick gold backings. For bombardment the targets were positioned at the end of the tube at an angle of 45^{o} with respect to the beam and maintained in vacuum by an O-ring seal. Direct water cooling of the targets made it possible to run beam currents of 6 - 10 μamps on the targets without any noticeable deterioration of the target material over periods of 24 hours or longer. A gate-valve, which isolates the target from the main beam tube, facilitates quick target changes.

The γ-ray detector used in these experiments to study the γ-rays from the decay of resonant states and the Doppler-shift measurements was a 60-cm^3 Ge(Li) coaxial (one end closed) detector mounted in a standard commercial cryostat. The Ge(Li) detector was mounted on one of the movable arms of a 48-in. diameter scattering table. A $2\frac{1}{4}'' \times 2\frac{1}{4}''$ NaI(Tℓ) scintillation counter was mounted on the other movable arm. The NaI counter was used for measuring the yield curve (excitation function) of the reaction $^{29}Si(p,\gamma)^{30}P$. The NaI count rate was also monitored with a scaler as a check on target deterioration. A schematic diagram of the electronics used is shown in Figure 3. Pulse-height analysis was accomplished with a 4096-channel NS-624 Analog-to-Digital converter.

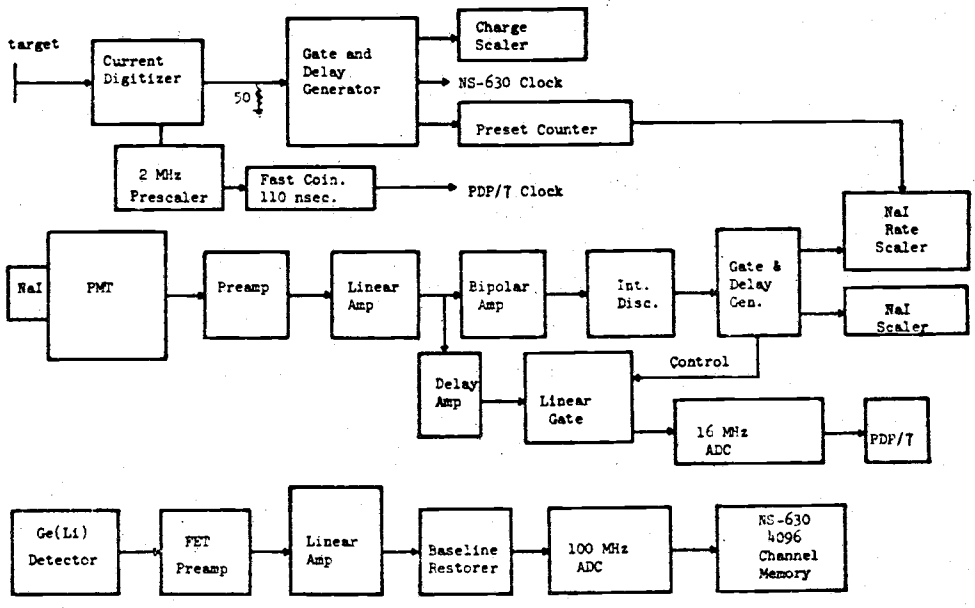

Fig 3 SCHEMATIC DIAGRAM OF THE ELECTRONICS USED.

Events are stored in the 4096-channel NS-630 analyzer memory unit and then transferred to a PDP-7 digital computer with display and spectrum analysis software capability. Final data storage is made on a magnetic tape.

3.2. Relative Efficiency Calibration

The relative photopeak efficiency of the 60-cm^3 Ge(Li) detector, which had a resolution of 2.4 KeV FWHM for the 1332 KeV ^{60}Co peak, was determined as a function of the γ-ray energy from the measured photopeak areas and the well-known relative intensities of γ-rays from a ^{56}Co source (50). The efficiency ratio of two γ-rays of energies E_1 and E_2 is related to the ratio of the areas and their relative intensities in the source in the following form:

$$\frac{\epsilon_1}{\epsilon_2} = \left(\frac{N_1}{N_2} \right) \left(\frac{I_2}{I_1} \right),$$

where $\frac{\epsilon_1}{\epsilon_2}$, $\frac{N_1}{N_2}$, and $\frac{I_1}{I_2}$ are the ratios of the efficiencies, peak areas and intensities respectively for the two γ-rays. When the Ge(Li) detector is used in the energy region above 2 MeV, the most important peak in the spectrum is the double-escape peak of energy $(E_\gamma - 2m_e c^2)$. Therefore, it is very useful to know the efficiency with which this peak is detected. In the case of ^{56}Co isotope, the

relative number of counts in a double-escape peak and the corresponding photopeak gives directly the relative double-escape peak and photo-peak efficiencies up to 3.5 MeV. The double-escape peak efficiency for γ-ray energies above 3.5 MeV was obtained using the γ-rays from the proton capture reactions $^{27}Al(p,\gamma)^{28}Si$ at $E_p = 1262$, 1589, and 2319 KeV and $^{39}K(p,\gamma)^{40}Ca$ at 1486 and 1666 KeV. In each case a single high energy γ-ray populated a low-lying energy level. In this simple cascade, when there are no competing transitions into or out of the intermediate level, the two cascade γ-rays have the same intensity. The ratio of the areas under the two corresponding peaks in the spectrum then directly gives the ratio of efficiencies. The measurements were normalized to the full-escape peak efficiency using the ratio of full-escape peak and double-escape peak areas for gamma rays below 4 MeV.

The relative efficiency curves for the photopeak and the double-escape peak are shown in Figure 4.

For the determination of γ-ray intensities, γ-ray spectra were recorded at $\theta = 55^{\circ}$ relative to the beam axis. At $\theta = 55^{\circ}$, the angular distribution effects are minimized, since the $P_2(\cos\theta)$ term in the angular distribution function is zero and the higher terms are considered to be very small. The peak areas needed for relative intensity determinations were found by using the computer code "GASPAN." This program locates peaks in a spectrum, fits each

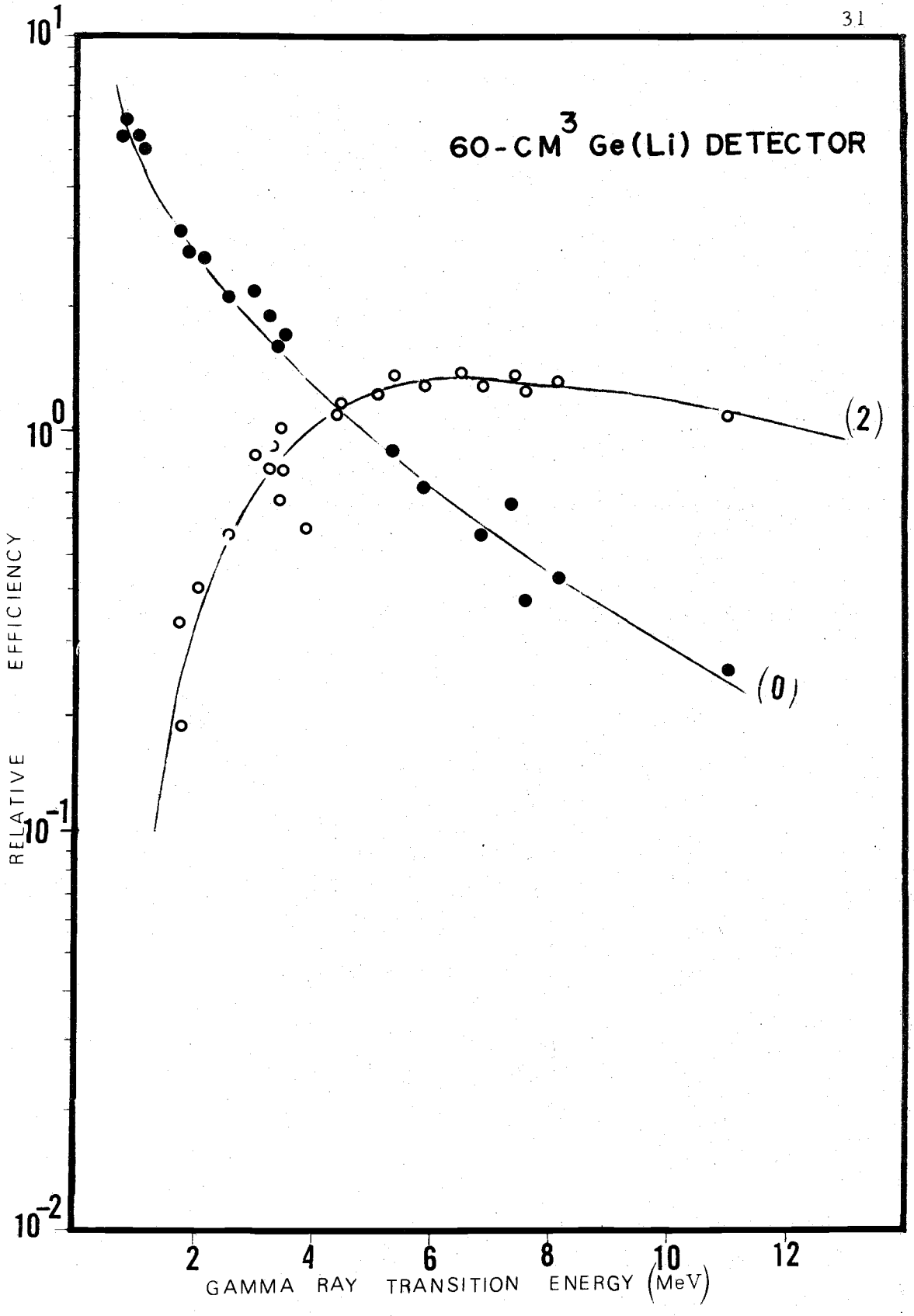

Fig.4 RELATIVE EFFICIENCY CURVE.

one to a Gaussian plus a linear background, and calculates the net number of counts above the background under each peak.

3.3. Gamma Ray Measurements

Precision measurements of γ-ray energies from the $^{29}Si(p,\gamma)^{30}P$ reaction were made at five resonances corresponding to proton bombarding energies of E_p = 2040, 2084, 2125, 2229, and 2410 KeV. In all cases the measured γ-ray energies were corrected for recoil of the compound nucleus due to photon emission. A computer code "DERIV" was used to convert the peak positions (channel numbers) into energies. In this program, the calibration curve (energy vs. peak position) is developed into a power series, and for its construction a least square fitting procedure is used with the following constraints:

1) the 511.006 KeV differences between the full energy, single escape, and double escape peaks of prominent transitions in each spectrum, and
2) the positions of the 511.006 KeV annihilation radiation peak, the 1460.75 KeV γ-ray from $^{40}K(\beta^+)$, the 2614.47 KeV γ-ray from ThC"and 6129.3 KeV γ-ray, and its double-escape peak, from the reaction $^{19}F(p,\alpha\gamma)^{16}O$.

In all cases, a cubic fit was found to be quite satisfactory.

To establish the decay scheme of each resonance, γ-ray

spectra were recorded for 6 - 8 hours with the detector located at 55^{o} with respect to the beam direction. Because of the high quality of the energy resolution of the detector, the simple condition that the energies of transitions in a cascade add up to the resonance level excitation energy, was quite powerful in the determination of decay schemes. An additional requirement was that the intensity of primary transitions equal or exceed the sum of the intensities of the observed secondary transitions.

The level energies of the levels of ^{30}P populated in the γ-decay of the resonant states corresponding to E_p = 2040 and 2125 KeV were determined by taking the γ-spectra at $\theta = 90^{o}$ with respect to the proton beam direction. In this geometry, the energy of the γ-rays incident at the detector is not Doppler-shifted. In all cases the measured γ-ray energies were corrected for recoil of the residual nucleus due to photon emission.

3.4. DSA Measurements

The DSAM measurements were made with the 60-cm^3 Ge(Li) detector located at 0^{o}, 90^{o}, and 120^{o} relative to the incident beam direction, using 10 - 12 KeV thick ^{29}SiO targets on gold backings. This target thickness was considered to be enough to stop the recoiling nuclei in the target deposit and not partly in the backing material. Typical measurements lasted 7 - 12 hours at an average beam current

of 7 μamps. The distance of the detector from the target was about 10 cm.

At E_p = 2040 KeV bombarding energy, the γ-spectra were recorded alternately at $\theta = 0^\circ$ and $\theta = 120^\circ$ with respect to the beam. Data were collected for 42 hours ($\approx$ 7 hours at each angle). The dispersion was 1.1 KeV/ch. For determining the Doppler-shifts, averages of the three spectra at each angle were taken. In many cases the double-escape peaks were also used in determining the Doppler-shifts. At E_p = 2125 and 2410 KeV, the γ-ray spectra were recorded at $\theta = 0^\circ$ and 120° using the same target as used for E_p = 2040 KeV measurements. The dispersion was $\approx$ 0.9 KeV/ch.

Fresh targets were then used at E_p = 2125 and 2410 KeV and γ-ray spectra were recorded at $\theta = 0^\circ$, $\theta = 90^\circ$ for the 2125 KeV resonance, and $\theta = 0^\circ$, $\theta = 120^\circ$ for the 2410 KeV resonance. The dispersion used was $\approx$ 0.5 KeV/ch. Gamma-ray spectra were recorded for 12 hours at each angle.

Errors in the analysis of Doppler-shift measurements are caused by the uncertainty in peak centroid determinations and by the uncertainty in the determination of zero and gain shifts between measurements at two different angles. Protection of the equipment from vibrations, while moving the detector from one angle to the other, is essential to gain stability. The centroid error was identified with the standard deviation of the corresponding parameter in the least squares

fitting of the γ-ray peak. The zero and gain shift corrections were found from the measured shifts of γ-rays that are known to be unshifted in energy (because of long lifetimes), such as 1460.75 KeV from $^{40}K(\beta^+)$, 2614.47 KeV from ThC'', and 6129.3 KeV from the reaction $^{19}F(p,\alpha\gamma)^{16}O$, and from the shifts of peaks whose lifetimes are so short as to give a full Doppler-shift (e.g. resonance transitions). The error was then associated with the average deviation of these points from the least squares fitted correction curve. Usually a linear fit was found to be quite adequate. The correction curve for zero and gain shifts for each resonance is shown in Figure 5.

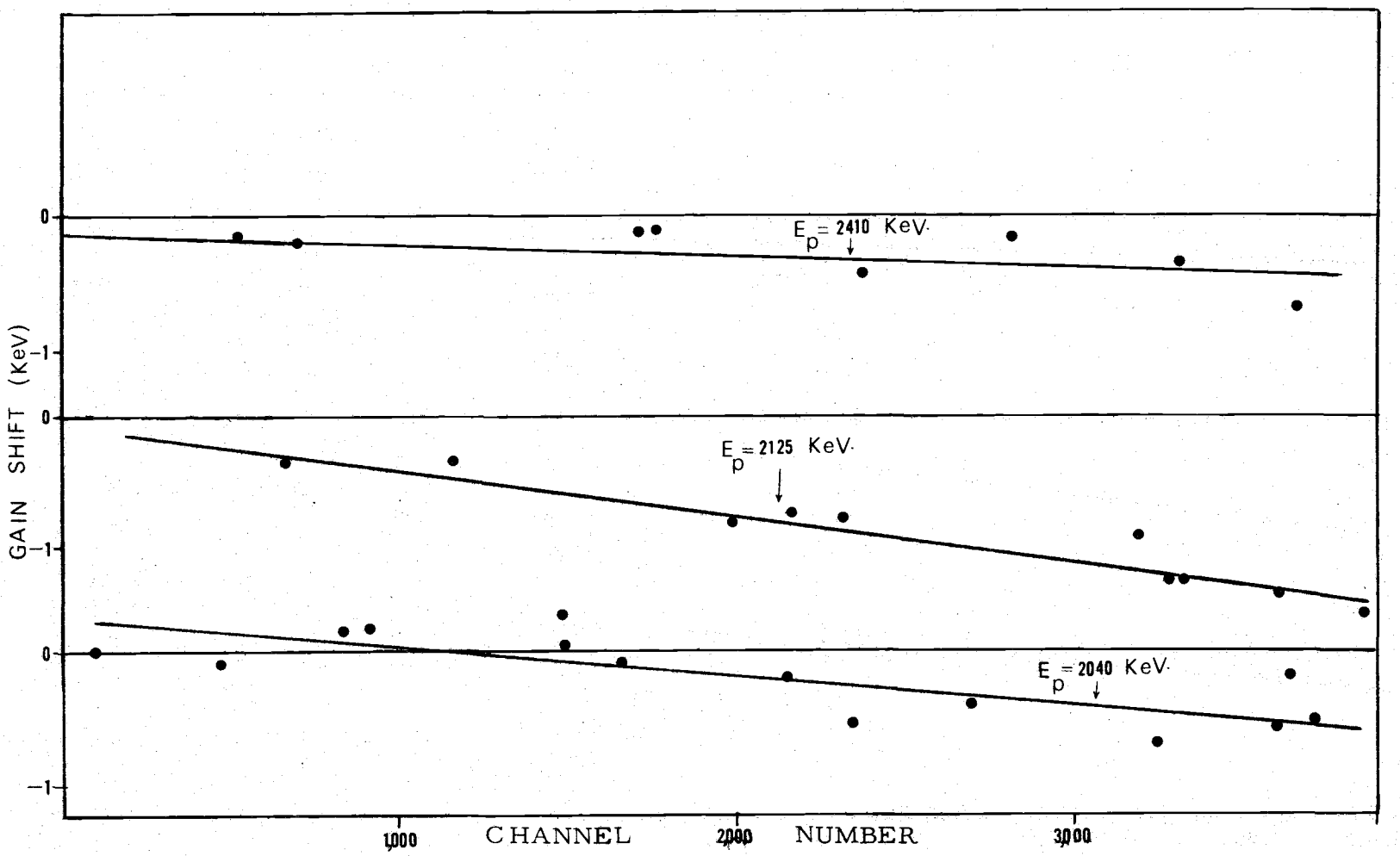

Fig.5 CORRECTION CURVES FOR ZERO AND GAIN SHIFT.

IV. RESULTS AND ANALYSIS

The measurements carried out in the present study of the $^{29}Si(p,\gamma)^{30}P$ reaction consisted of the following:

1) the yield curve (excitation function) in the energy range $E_p = 2.0$ to 2.5 MeV to locate the prominent resonances at $E_p = 2040$, 2084, 2125, 2234, and 2410 KeV,
2) the gamma-ray spectra from the decay of resonant states in ^{30}P corresponding to the above mentioned resonances, thereby establishing their decay schemes and branching ratios,
3) the excitation energies of the bound states and the reaction Q-value, and
4) the Doppler-shift attenuation measurements at 2040, 2125, and 2410 KeV resonances.

4.1. Yield Curve

The yield of the γ-rays from a 10 - 12 KeV thick $^{29}SiO_2$ target was observed with a $2\frac{1}{4}'' \times 2\frac{1}{4}''$ NaI(Tℓ) scintillation counter located at 55^{o} with respect to the incident proton beam direction. The detector was placed close to the target to reduce the effect of the background. A discrimination bias was set at 3 MeV so that only pulses corresponding to γ-ray energy greater than 3 MeV were accepted. This setting was high enough to exclude those pulses

arising from the relatively intense 1461 and 2614 KeV room background γ-rays. The bombarding energy was varied between 2 to 2.5 MeV in steps of 1 KeV or less near the previously reported locations of (p, γ) resonances, and in steps of 5 KeV in the regions of no resonance structure. The energy scale for the bombarding proton energies was calibrated by means of the strong $^{27}Al(p, \gamma)^{28}Si$ resonances at 991.88 ± 0.04 KeV (51) and 1118.4 ± 0.02 KeV (52). Figure 6 shows the γ-ray yield curve obtained for the reaction $^{29}Si(p, \gamma)^{30}P$ in the regions of the E_p = 2040, 2084, 2125, 2234, and 2410 KeV resonances. It agrees very well with earlier measurements (53, 54). The energies of these resonances are known within ±2 KeV. Recently, Poirier et al. (55) have reported precise energies of these resonances within ±0.5 KeV as follows:

2039.8 ± 0.5, 2083.8 ± 0.5, 2125.2 ± 0.5, 2234.1 ± 0.5, and 2410.6 ± 0.5 KeV.

4.2. Resonance Spectra

The spectrum of γ-rays originating from each of the five resonances at E_p = 2040, 2089, 2125, 2234, and 2410 KeV was observed with a 60-cm^3 Ge(Li) detector located at 55° relative to the beam direction. The resonances spectra were recorded for 5 - 7 hours with the detector placed at nearly 10 cm. from the target. Beam currents of 6 - 10 μamps. were maintained for periods up to

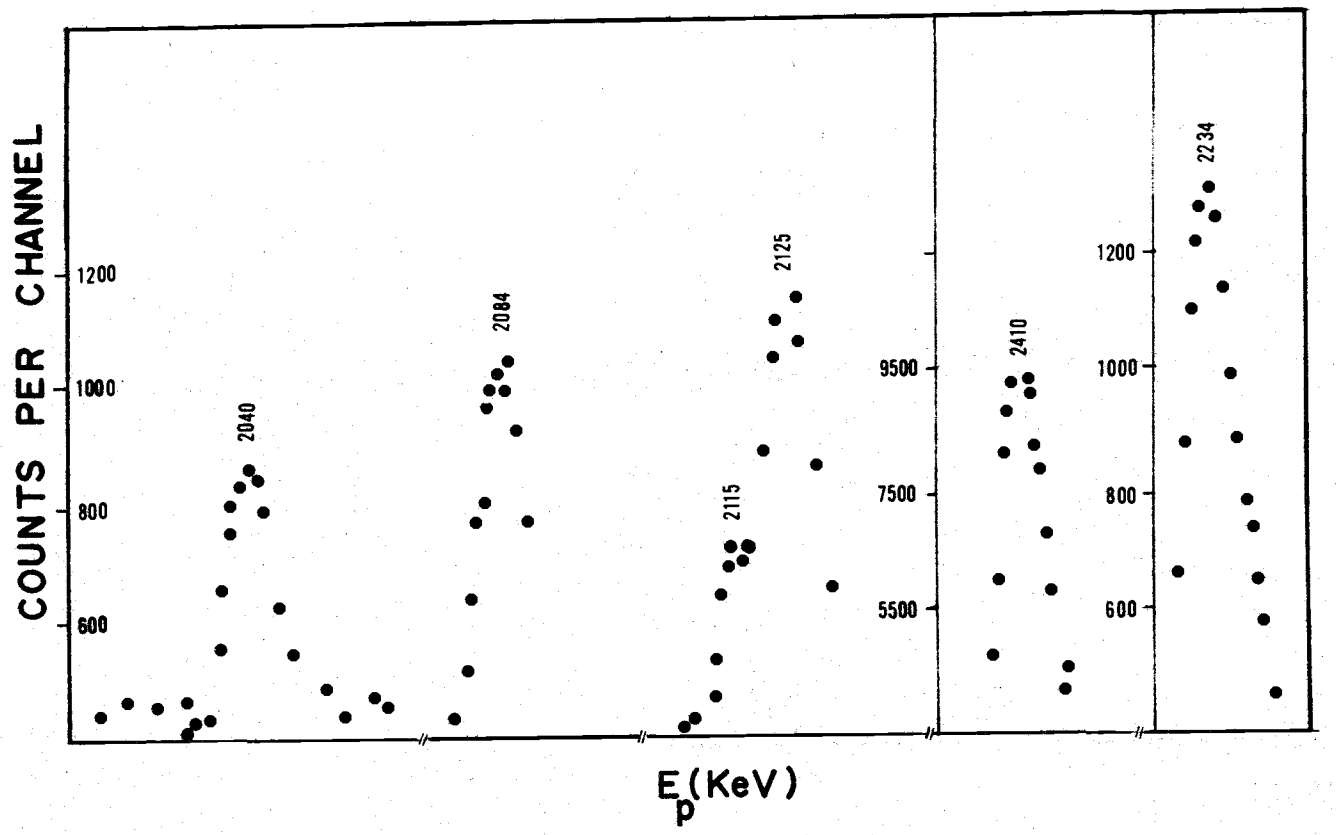

Fig. 6 YIELD CURVE FOR THE REACTION $^{29}Si(p,\gamma)^{30}P$ IN THE ENERGY REGION 2–2.5 MeV.

48 hours. The target backing was water-cooled and could withstand large currents over long periods of irradiation. The energy dispersion was about 2 KeV/channel. Typical resonance spectra obtained at E_p = 2040, 2084, 2234, and 2410 KeV are shown in Figures 7, 8, 9, and 10, respectively. A number of contaminant γ-rays appear in these spectra, e.g., 6129.3 KeV line from $^{19}F(p,\alpha\gamma)^{16}O$; 1460.75 KeV line from $^{40}K(\beta^+)$; 2614.47 KeV line from ThC''; 1273 KeV line from $^{29}Si(p,p')$; 1633 KeV line from $^{23}Na(p,\alpha\gamma)^{20}Ne$; 1368 KeV line from $^{27}A\ell(p,\gamma)^{24}Mg$ (which could also be assigned to the reaction $^{23}Na(p,\gamma)^{24}Mg$), and 440 KeV line from the $^{23}Na(p,p')$ reaction. The γ-rays at 6129.3 KeV and its double-escape peak, 2614 KeV, and 1461 KeV were found to be very useful as calibration points for the energy scale of the pulse height spectrum. The location of the peak centroids and energy calibration were carried out with computer programs as described in section 3.3.

The relative intensities of the transitions were derived from the relative photo-peak or the second-escape peak intensities using the relative efficiency curve shown in Figure 4.

The energies and intensities of the γ-rays at each resonance were used to construct a decay scheme for each resonance studied in this work. The decay schemes and the branching ratios for the resonances studied are presented in Table 2 and Figures 11, 12, 13, 14, and 15. The results of the earlier measurements are also given

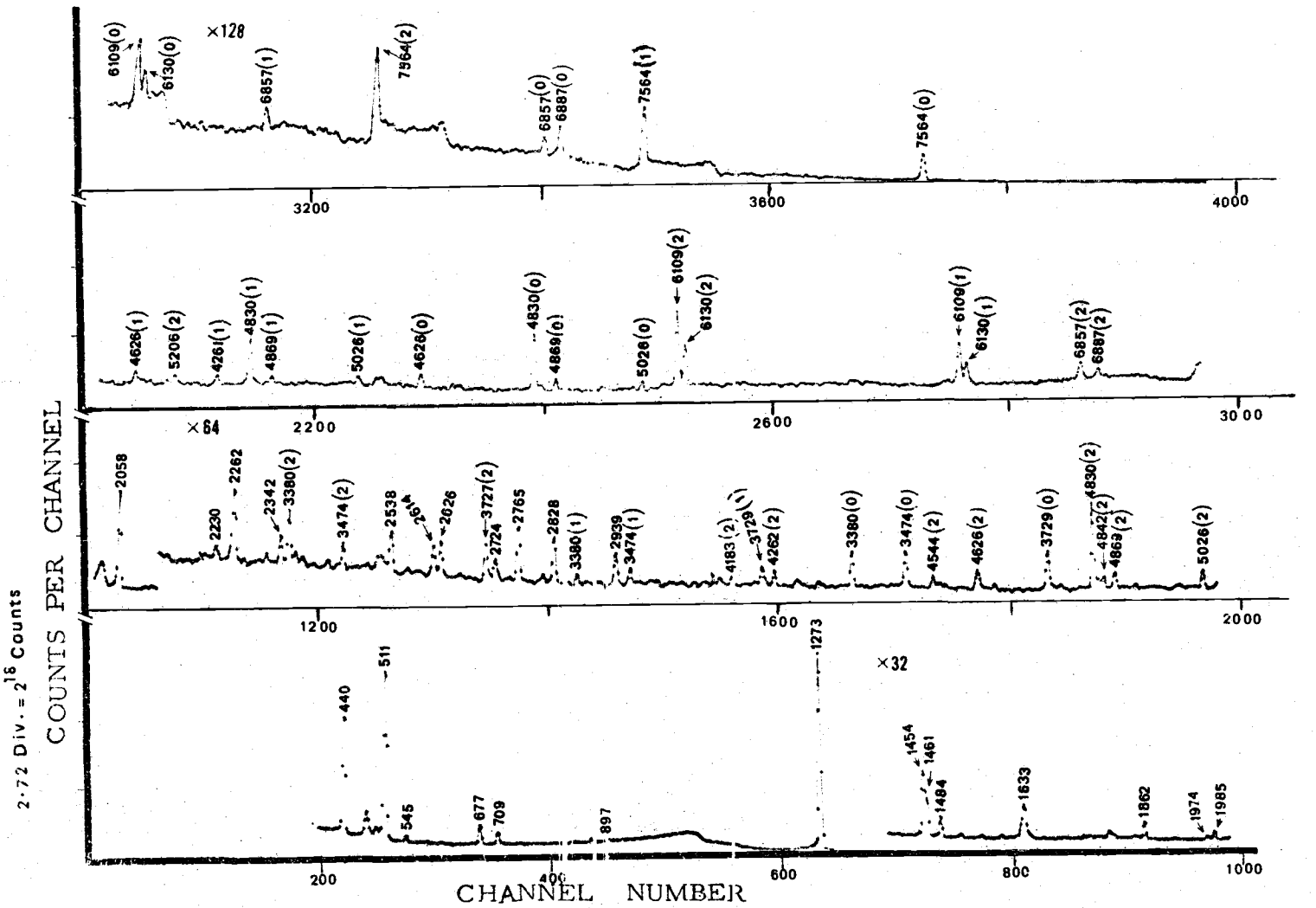

Figure 7. Gamma-ray spectrum of the 2040 KeV resonance at $\theta = 55^{\circ}$. The γ-energies are written above the peaks.

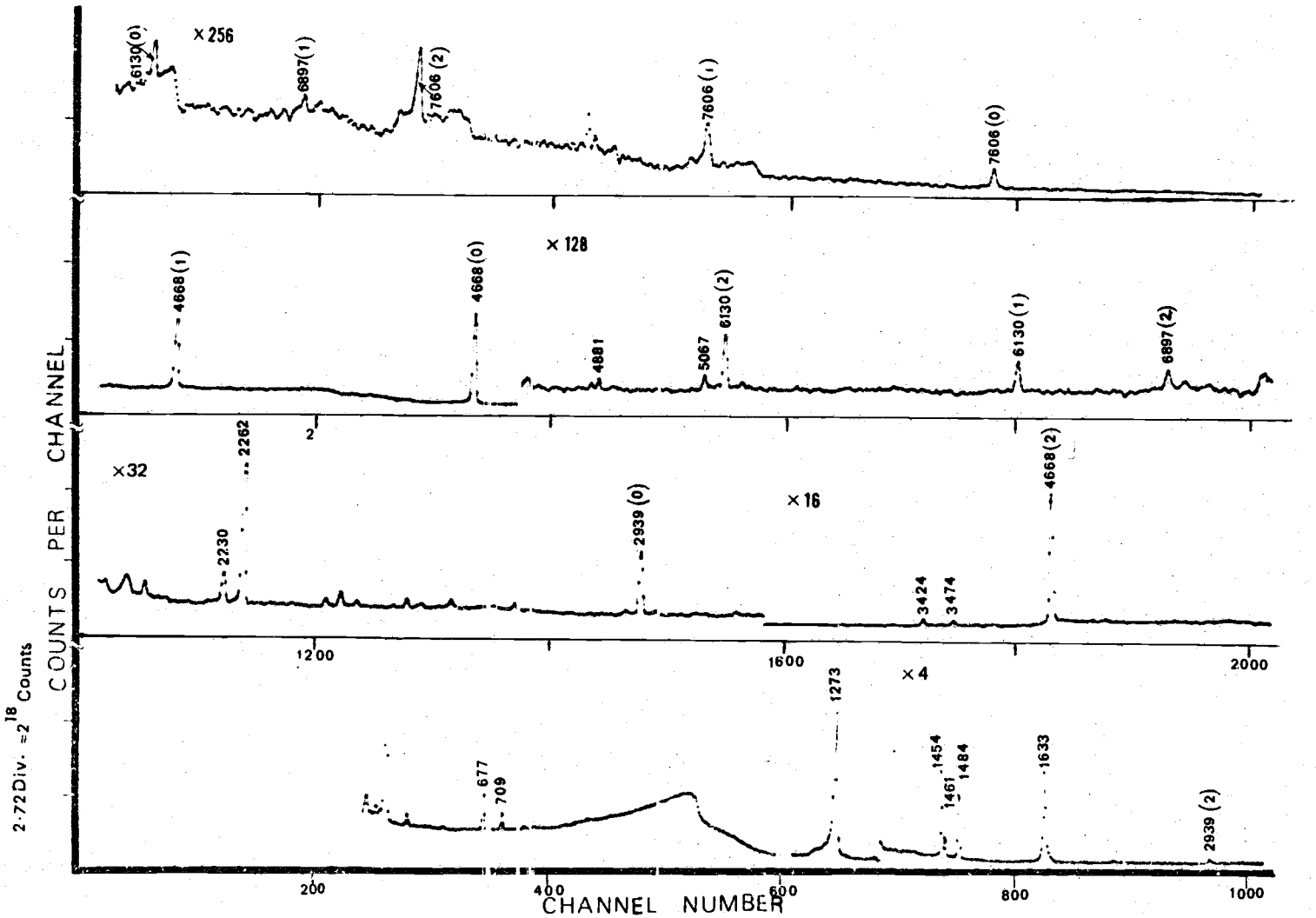

Figure 8. Gamma-ray spectrum of the 2084 KeV resonance at $\theta = 55^{\circ}$. The γ-energies are written above the peaks.

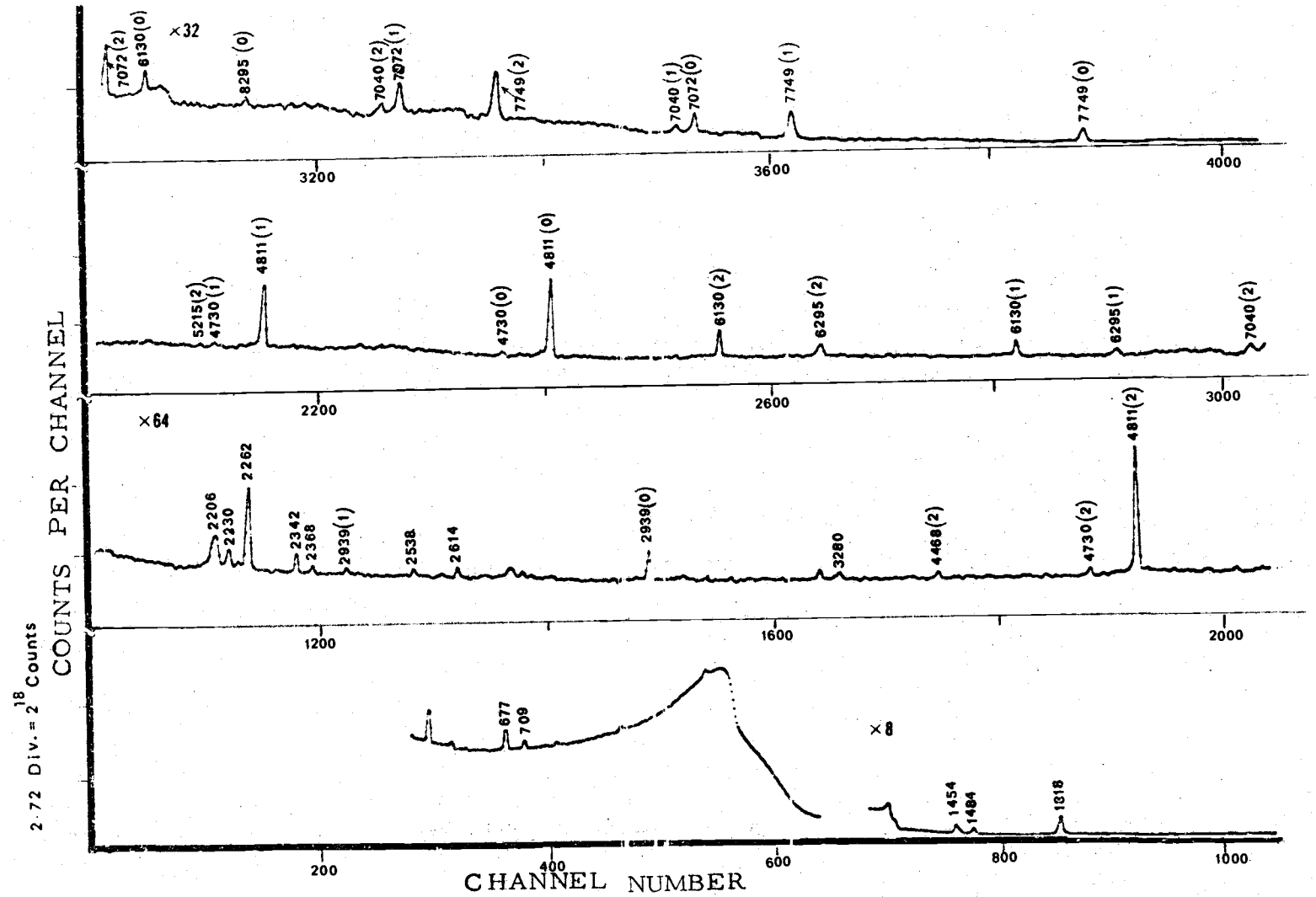

Figure 9. Gamma-ray spectrum of the 2234 KeV resonance at $\theta = 55^{\circ}$. The γ-energies are written above the peaks.

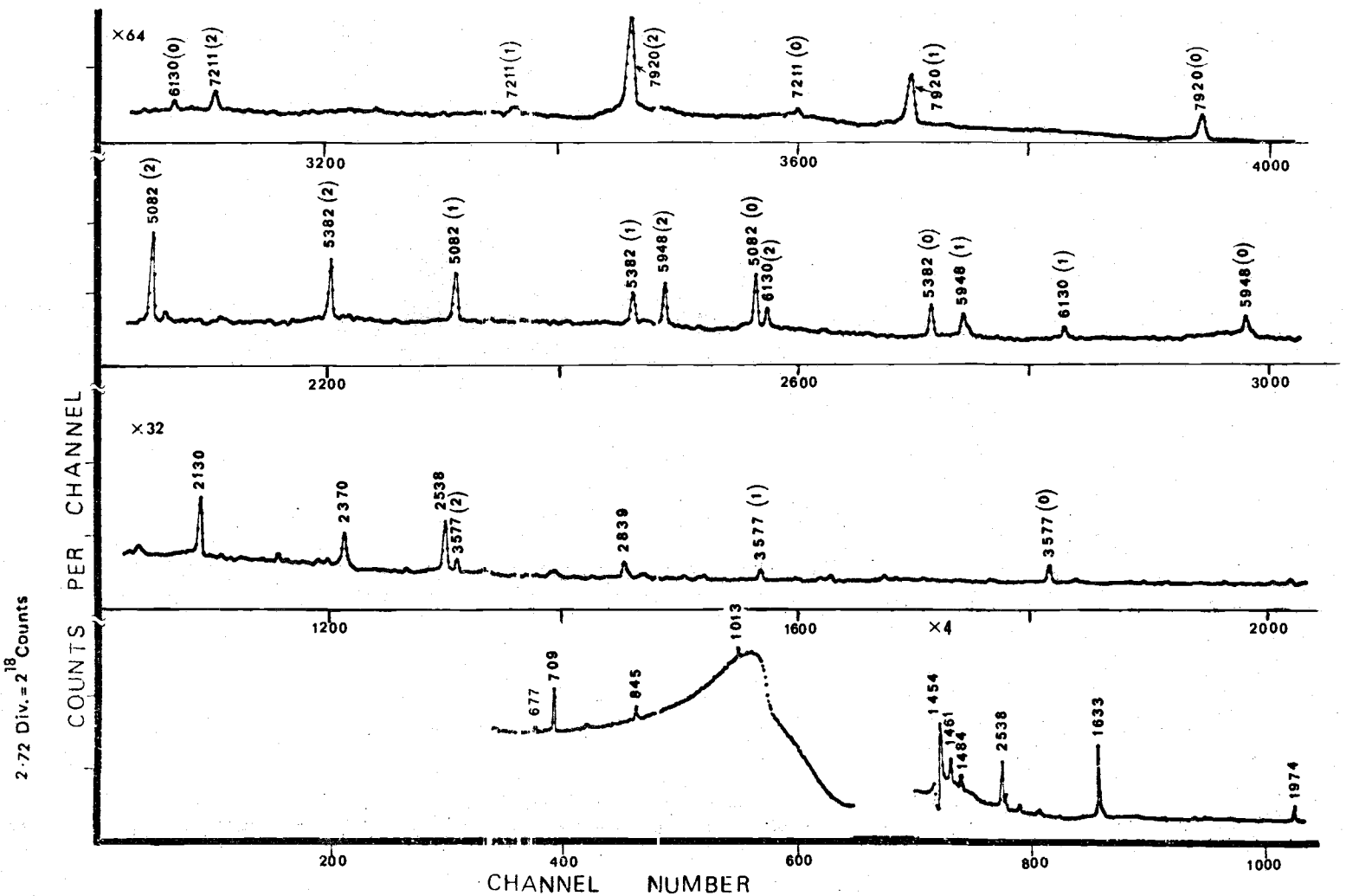

Figure 10. Gamma-ray spectrum of the 2410 KeV resonance at $\Theta = 55^{\circ}$. The γ-energies are written above the peaks.

Table 2. Relative Intensity of Gamma-rays in the Decay of Resonant States.

Transition from resonant state to final state (KeV)	Resonant state energy E_p (in KeV)				
	2040	2084	2125	2234	2410
0	11	3	3	16	36
677	2			13	
709	3	2		6	6
1454	15			7	
1974			3		11
2539	3	2	33	2	15
2724	3	1	10		
2839			7		21
2939	5	88	11	52	1
3020	2			4	1
3836	7		12		
4183	5	3	5		
4343					7
4422			5		
4736	6		11		2
4939	4				
5207	3				
5506	16				
5577	5				
5702	10				

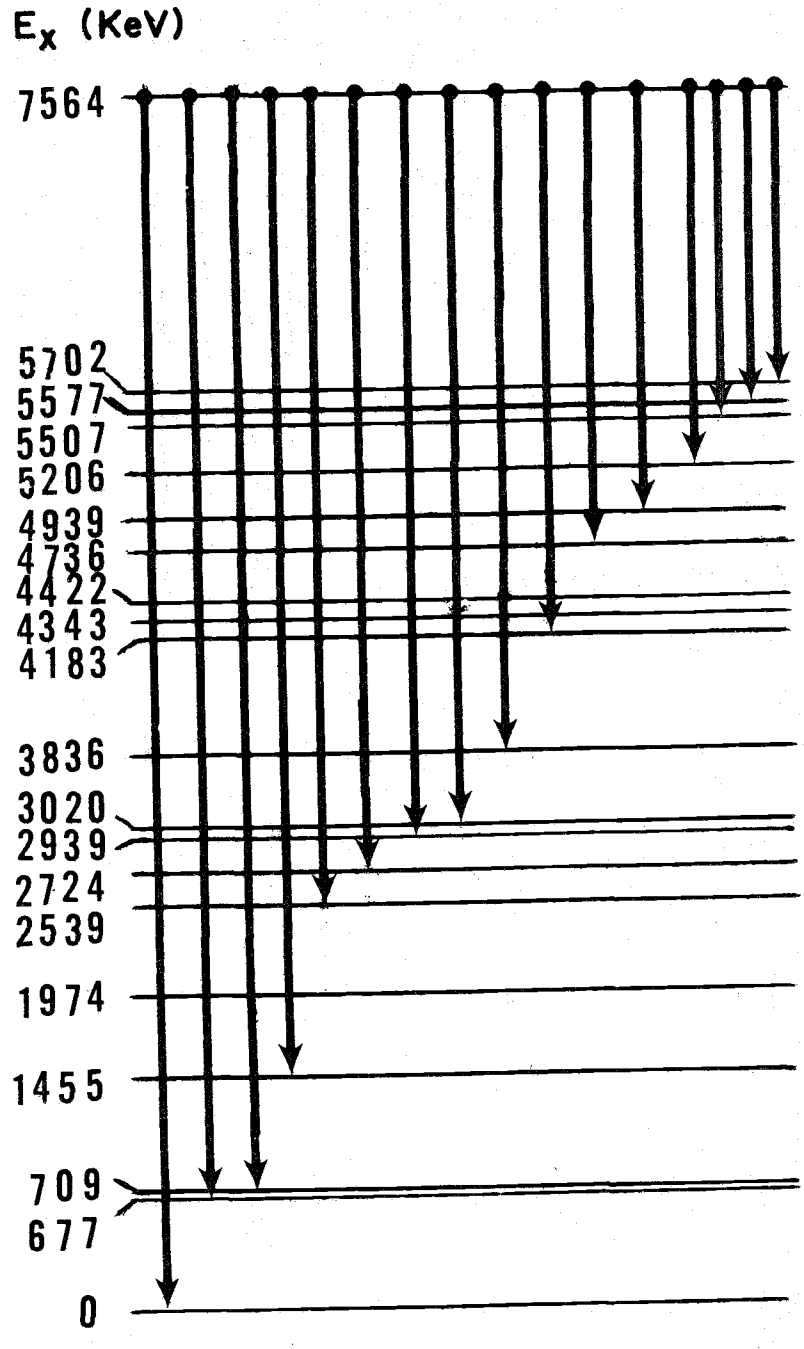

Fig. 11 DECAY SCHEME OF 2040 KeV RESONANCE

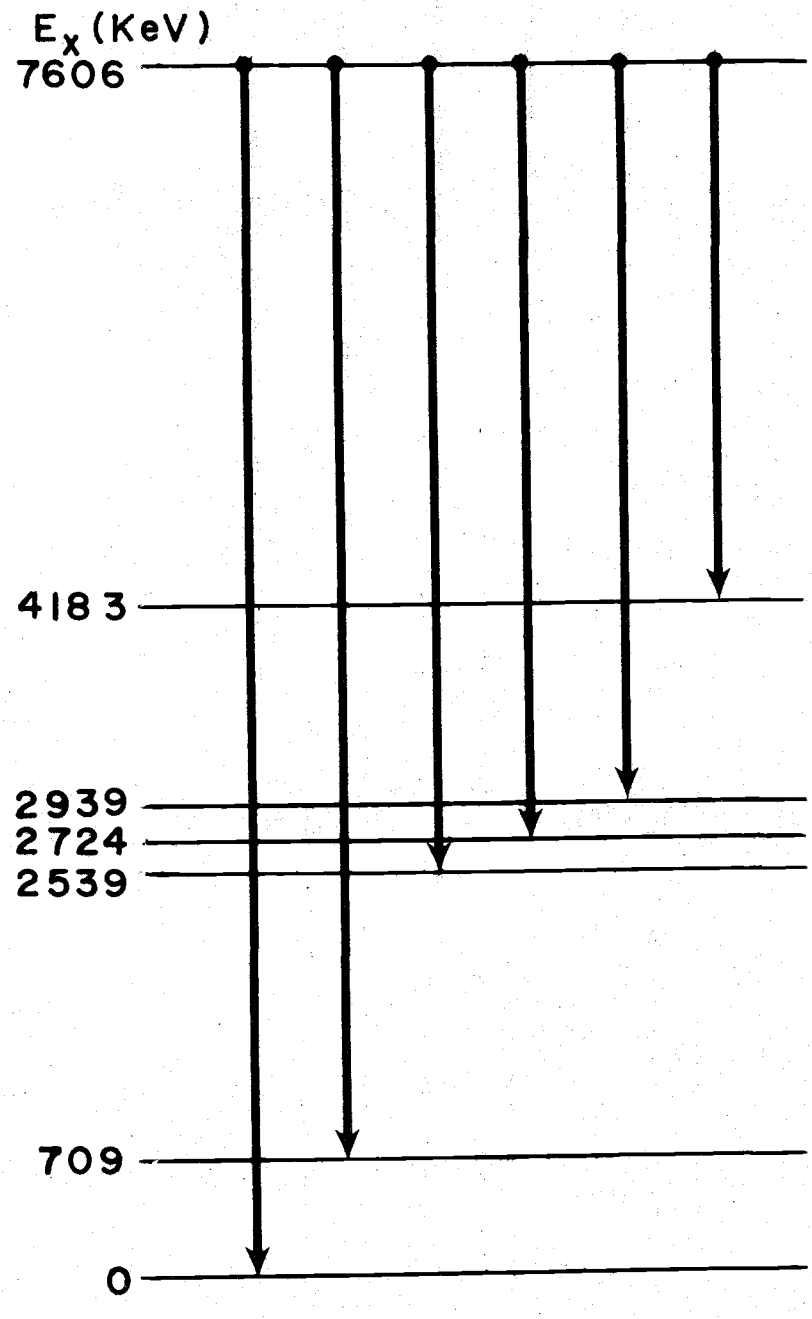

Fig. 12 DECAY SCHEME OF 2084 KeV RESONANCE

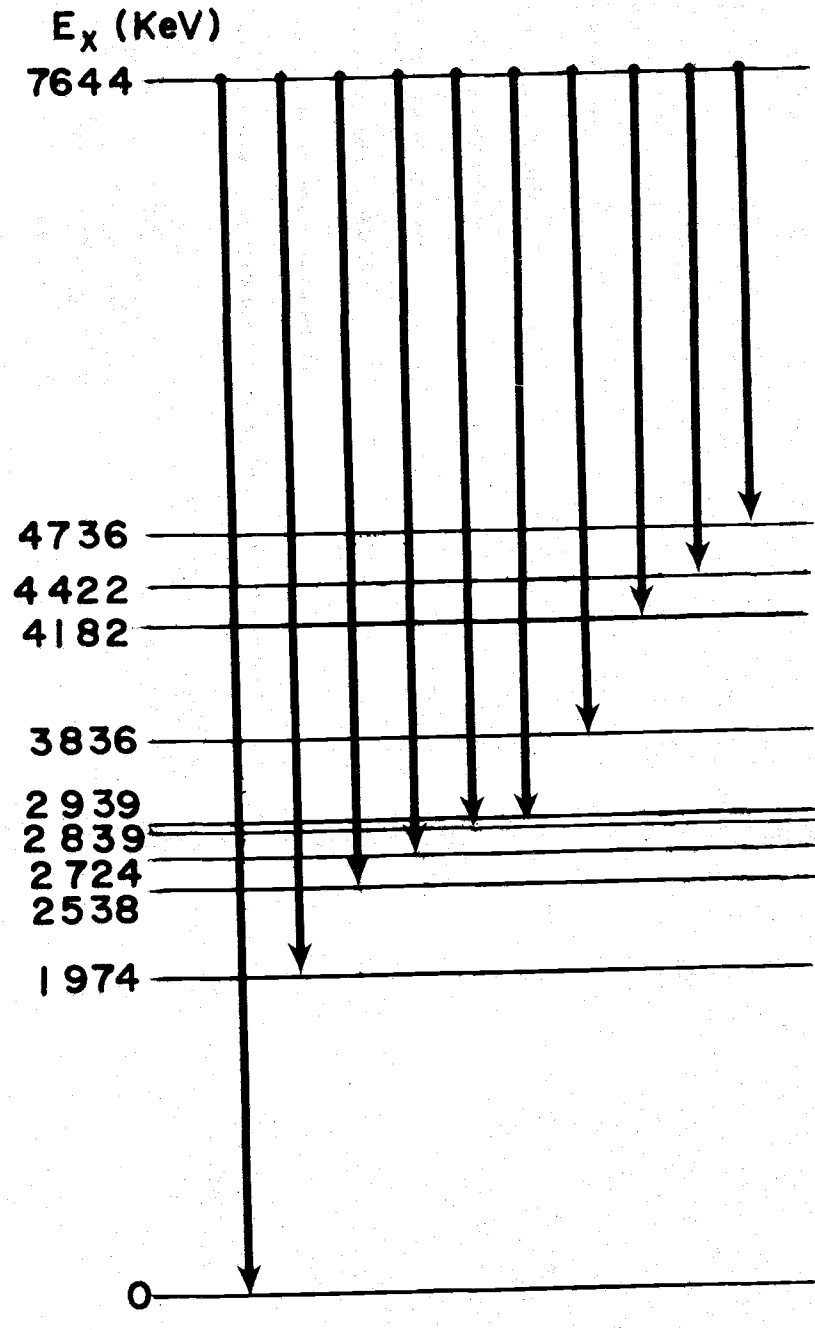

Fig. 13 DECAY SCHEME OF 2125 KeV RESONANCE

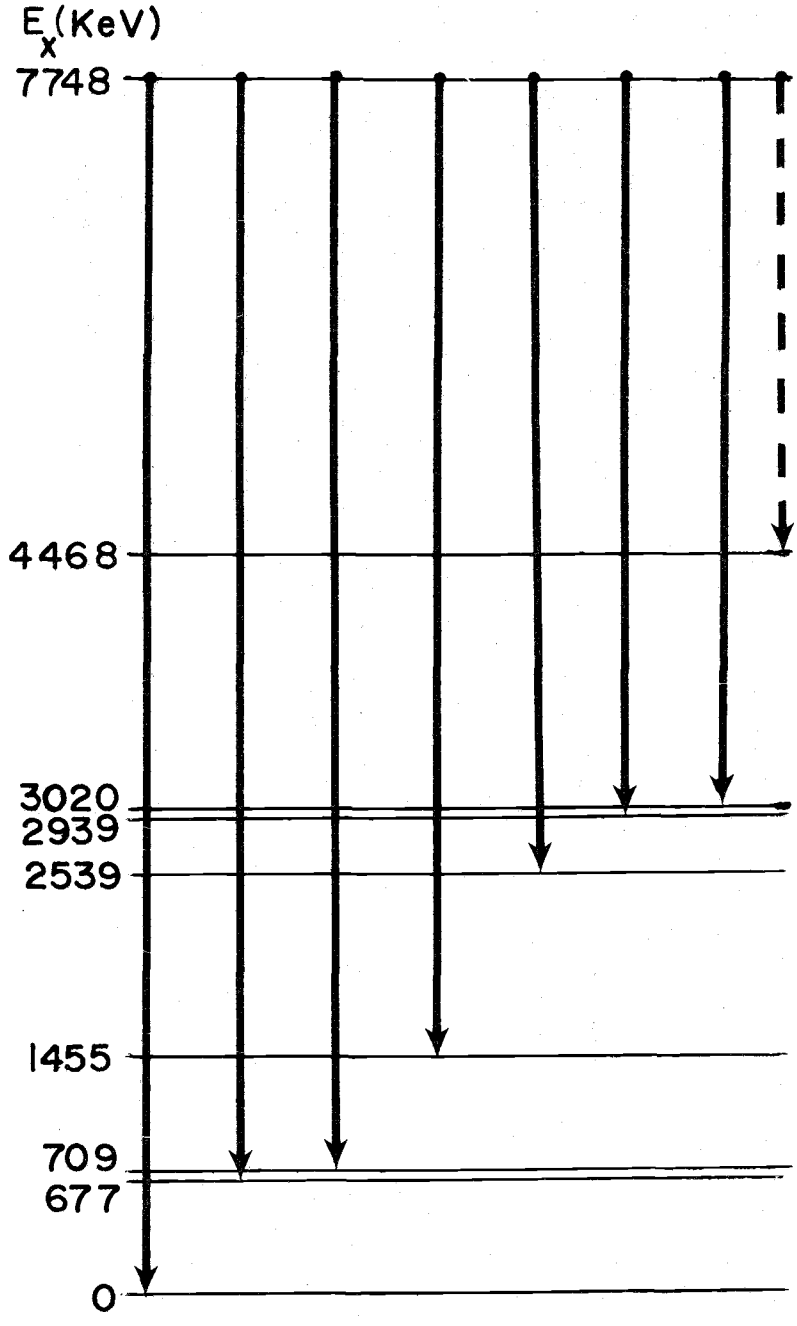

Fig. 14 DECAY SCHEME OF 2234 KeV RESONANCE

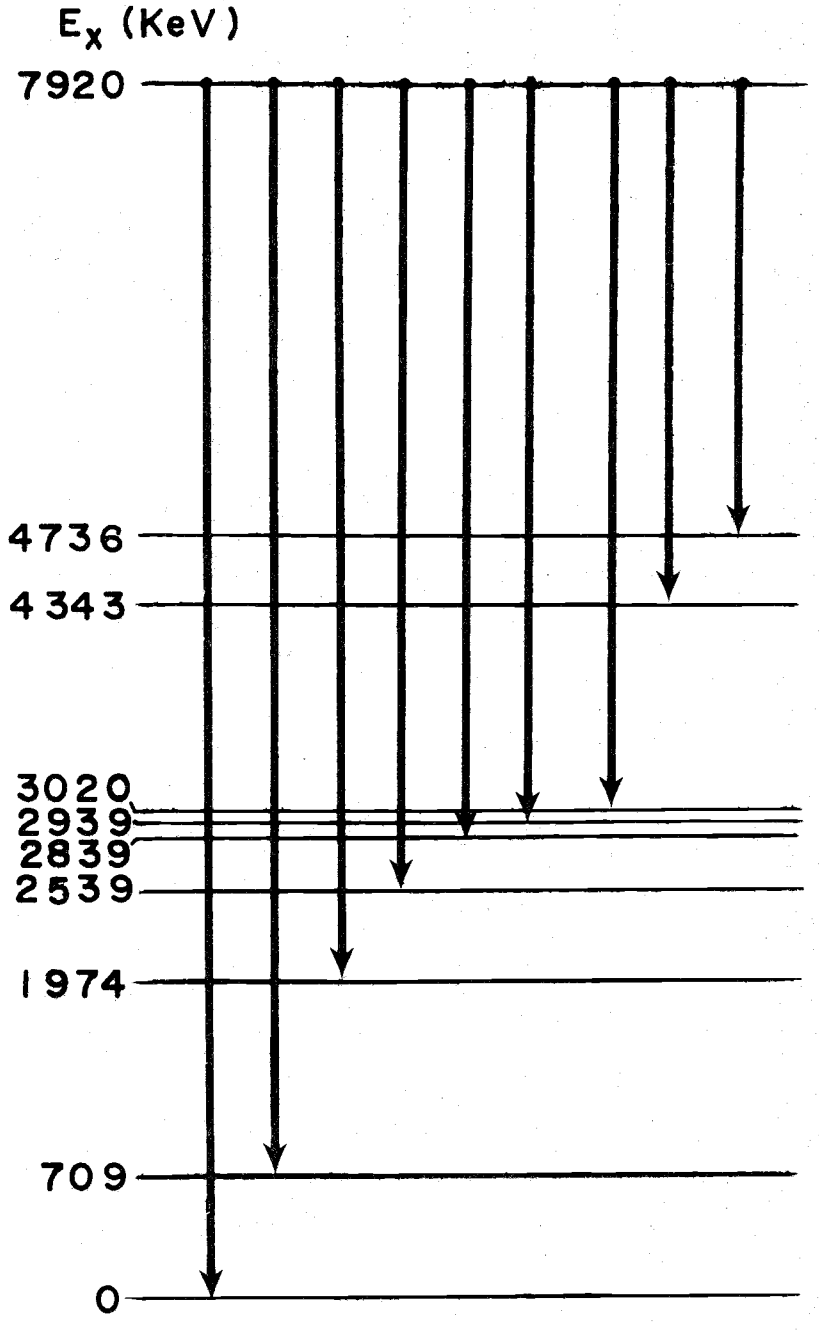

Fig. 15 DECAY SCHEME OF 2410 KeV RESONANCE

for comparison. When this work was started, there were two experimental studies reported (27, 30) for the γ-decay of the 2040 KeV resonance and only one (30) at E_p = 2084 and 2125 KeV resonances. There were no previous measurements at E_p = 2234 and 2410 KeV resonances. Recently, Kostin et al. (57) have reported the results of their investigations for the resonances in the energy region $2.0 \leq E_p \leq 2.5$ MeV. The main features of the different resonances studied in this work are as follows:

2040 KeV Resonance

The excitation energy of the resonance state, according to the Q-value determined in the present study, is 7564.0 KeV. Fifteen primary γ-rays were observed from the decay of this resonance state. This resonance is remarkable, as it decays to the bound levels at 3.84, 4.74, 4.94, 5.21, 5.51, 5.58, and 5.70 MeV excitation energy, which have either not been excited by the γ-decay of any other resonance or are populated at very few resonances. This resonance also decays to nine other bound levels in ^{30}P which are also excited at a number of other resonances. The decay to the bound level at 5.51 MeV excitation energy has been reported at only one resonance. Bergstrom - Rohlin (28) observed that the 1669 KeV resonance state decays 79% to the 3.02 and 21% to the 5.51 MeV level. Recently, Din and Davis (30) have reported that the levels at 4.74 and

3.84 MeV excitation energy are also populated by the deexcitation of 2115 and 2125 KeV resonances. The levels at 3.84, 4.74, 4.94, 5.21, 5.51, and 5.70 MeV, with the exception of 5.58 MeV level, had previously been seen in the $^{32}S(d, \alpha)^{30}P$ reaction by Endt and Paris (18).

The previous data on 2040 KeV resonance is that of Din and Davis (30), and that of Phelps et al. (27) who observed only a 5.10 MeV γ-ray at this resonance. The results of the present investigation of the 2040 KeV resonance are generally in good agreement with those of Din and Davis, except for the slight differences in the relative intensities of different transitions. Din and Davis reported the relative intensities of the transitions to the 1454, 2939, 3836, 4183, 4940, and 5506 KeV levels to be 13, 3, 10, 1, 8, 6, 22 percent, respectively, whereas in the present investigation the relative intensities of the transitions to these levels were found to be 15, 5, 7, 5, 6.4, and 16 percent, respectively. In the present investigation, two additional weaker γ-rays at 4.87 and 1.99 MeV energy were observed in the γ-ray spectrum. These γ's appeared only at E_p = 2040 KeV, and not in the decay of the other resonances studied i.e. at E_p = 2084, 2125, 2234 and 2410 KeV resonances. These two gammas can be accounted for if it is assumed that the 4.87 and 1.99 MeV γ-rays result from a cascade through a level at 5.58 MeV and the known level at 0.71 MeV. A level at 5598 $\pm$ 10 KeV has been observed by Endt and Paris

in the study of the reaction $^{32}S(d, \alpha)^{30}P$.

Recently, Kostin et al. (57) have reported the results of their investigation of the 2040 resonance. They observed only six primary γ-rays compared with 14 - 15 primary gammas observed in the present study and also by Din and Davis (30). They reported 31, 18, and 22 percent transitions to the ground state 677, 1454 KeV levels respectively, whereas 10, 2, and 16 percent transitions were observed to these levels in the present investigation. In addition, they reported 6, 1 and 22 percent transitions to 3736, 1974 and 2724 KeV levels. Transitions to the 3736 and 1974 KeV levels were not observed in the present study, while the transition to the 2724 KeV level was observed to be only 3 percent. Din and Davis did not observe the feeding line to this level, although they observed the 2724 γ-ray.

2084 KeV Resonance

This resonance state at 7607 KeV excitation energy decays strongly (88 percent) to the 2939 KeV level, with very weak transitions to the ground state and 709, 2539, 2724 and 4183 KeV levels. These observations are in excellent agreement with those of Din and Davis (30), but in disagreement with those of Kostin et al. (57). They reported a strong 87 percent transition to 2939 level, 12 percent decay to the ground state and 1 percent to the 2839 level, whereas in

the present investigation 4, 2, 2, 88, 3 and 1 percent transitions were observed to the ground state and to the 709, 2539, 2939, 4183 and 2724 KeV levels, respectively. No transition was observed to the 2839 KeV level.

2115 - 2125 KeV Resonances

The resonances at E_p = 2115 and 2125 KeV were not resolved in this work due to the thick target (10 - 12 KeV) used. However, primary transitions, differing in energy by about 8 KeV, were seen in the γ-ray spectrum indicating that the primary transitions were originating from two resonances, about 8 KeV apart, to the bound states in ^{30}P. The decay of the two resonances is identical. Both resonances decay strongly to the 4736, 4422, 4183, 3836, 2939, 2839, 2724, 2539 KeV levels, with weaker transitions to 1974 KeV level and to the ground state.

These results are in agreement with those of Din and Davis but in disagreement with those of Kostin et al. (57). They reported 7 percent decay to the 4142 level, which was neither reported by Din and Davis nor observed in the present study. No transitions to the ground state and to the 4422, 4736, 3836 levels were reported by Kostin et al.

2234 KeV Resonance

The two resonances at E_p = 2234 and 2242 KeV were not resolved because of the thick target used. Gamma decays to the 2939, 677, 709, 1454, 3020 and 2539 KeV levels in ^{30}P were observed. There is also some evidence of a weak transition to the 4468 KeV level. The decay to the 2939 KeV level is > 50 percent. Kostin et al. (57) have reported 80, 5, and 15 percent transitions to the 2939, 4183 KeV levels and to the ground state respectively. No transition to the 4183 KeV level was observed in this investigation. The sum of the γ-ray cascade transition energies lead to an excitation energy of 7751 KeV for the resonance level in all the observed transitions, which corresponds to E_p = 2234 KeV. Also, at the 2242 KeV resonance Kostin et al. reported a strong (>50 percent) transition to the 2724 KeV level. No such transition to the 2724 KeV level was observed. These observations indicate that the γ-rays in the spectrum are due mostly to the deexcitation of the 2234 KeV resonance.

2410 KeV Resonance

This resonant state at an excitation energy of 7922 KeV decays to the ground state and to the 2839, 2539, 4343, 1974, 709, 2939, 3020, and 4736 KeV levels. The transitions to the 2939, 3020, and 4736 KeV levels are less than 2 percent. The 4343 KeV level

previously seen in the $^{32}S(d, \alpha)^{30}P$ reaction by Endt and Paris (18), has not been reported in any other (p, γ) resonance experiment. Kostin et al. have reported transitions to the 1454, 1974, 2539, and 2839 KeV levels. The transition to the 1454 KeV level was not seen in this work. The branching ratios are also in disagreement with those reported by Kostin et al.

4.3. Excitation Energies of the Bound States and the Reaction Q-Value

To obtain accurate energy values for the bound states in ^{30}P, and to eliminate the broadening and shift of the gamma peaks due to the Doppler effect, single γ-ray spectra of the resonances at E_p = 2040 and 2125 KeV were taken at $\theta = 90^{o}$, where θ is the angle between the beam and the detector axis. In determining the energies of the bound states, correction associated with the recoil energy lost to the residual nucleus upon emission of the γ-quanta was taken into account.

A computer program "DERIV" was used to determine the energies of the peaks in the pulse-height spectrum. The input data for this program were accurately known energies of the room background γ-rays, namely 1460.75 ± 0.06 KeV (4) from $^{40}K(\beta^{+})$ and 2614.47 ± 0.10 KeV (5) from ThC", 6129.3 ± 0.4 KeV (3) and its double-escape peak from the reaction $^{19}F(p, \alpha\gamma)^{16}O$, energy separations between full-energy, single-, and double-escape peaks. In some

spectra γ-ray lines at 1173.23 ± 0.04 (58) and 1332.483 ± 0.046 (58) KeV from a ^{60}Co source were also included. Peak positions (channel numbers) were fitted with a polynomial in the γ-ray energy. Most spectra could be fitted well with a third degree polynomial.

This calibration procedure was checked by calibrating the low energy parts of the spectra with a ^{56}Co source (59). A γ-ray spectrum of the ^{56}Co source was taken with the same electronic settings as used for the 2040 KeV resonance γ-ray spectrum. The calibration curves were third degree polynomial expansion of channel numbers, and the parameters were determined from a least square fit. In this way it was possible to reach the double-escape peak of the 4251.1 KeV γ-ray. Calibration for higher energy γ-rays was achieved by iteration, that is by using the 4251.1 KeV γ-ray as input, it was possible to reach still higher γ-rays. Finally, the calibration peaks in the region 511.006 to 7570 KeV were used as input data and the energies of all peaks in the spectrum were calculated. The agreement between the two procedures was excellent. The excitation energies of the ^{30}P levels populated in the decay of 2040 and 2125 KeV resonances are given in Table 3. The excitation energy values are averages of all measurements weighted inversely as the squares of the uncertainties. The energy errors are taken as the larger of the systematical or statistical errors. For comparison the results of some of the previous measurements are also included.

Table 3. Excitation Energies (KeV) of ^{30}P Levels.

Present work	Ref. 18	Ref. 29	Ref. 35	Ref. 36
0	0	0		
677.4±0.5	680±2	684±3	677.0±0.5	
709.2±0.5	709±2	705±3		
1454.6±0.5	1453±2	1451±10	1454.0±0.5	
1973.7±0.7	1974±2	1972±10	1972.8±1.0	
2539.2±1.0	2536±2	2538±10	2538.2±0.7	
2724.0±0.5	2722±2	2723±10	2723.3±0.5	
2839.9±1.0		2839±10	2838.8±1.0	
2938.2±1.0	2939±2	2937±10	2937.5±1.0	
3020.1±0.5	3020±3	3018±10	3018.4±1.0	
	3736±3	3734±10		3729.2±1.5
3826.2±1.2		3836±10		3834.3±1.3
	3928±4	3926±10		3927.2±1.3
	4142±2	4141±10		4144.3±1.3
4183.2±1.2	4182±4	4181±10		4182.7±1.5
	4231±2	4230±10		4229.9±1.3
				4234.5±1.8
		4296±10		4298 ±5
		4343±10		4342.8±1.0
4422 ±2.0	4425±3	4421±10		
	4468±3			
	4501±3	4501±10		
	4624±2	4625±10		4624.9±1.5
4736.7±1.0		4734±10		
	4921±2	4929±10		
4938.5±1.0	4945±3			
		5024±10		
5206.6±2.0		5200±10		
		5410±10		
5507.1±1.0		5504±10		
5576.9±2.0		5598±10		
5702.3±1.0		5700±10		
		5790±10		

For the determination of the Q-value of the $^{29}Si(p,\gamma)^{30}P$ reaction, the sum of the 2-step, 3-step, and 4-step cascade transition energies accurately measured at E_p = 2040 KeV resonance were used to determine the excitation energy of the resonant state. This resonance exhibits a number of strong cascade transitions. Since the low energy γ-rays can be calibrated precisely, this permitted a more accurate determination of the excitation energy of the resonant state and, hence, the reaction Q-value, than previously known. The cascade γ-ray transition energies used for the determination of the resonance excitation energy are listed in Table 4. The resulting mean value for the excitation energy of the resonance level is 7564.0 ± 3 KeV. The corresponding Q-value determined from the excitation energy of the resonance state and the incident center-of-mass energy is given by:

$$\text{Q-Value} = \text{Excitation energy of the resonance} - E_{cm}(P)$$

$$= E_x - \frac{m}{M} E(p),$$

where m is the proton mass, M is the mass of the compound nucleus, and E_p is the energy of the incident proton in the lab-frame.

The Q-value is 5591.5 ± 3 KeV. The largest contributing error is usually the uncertainty of the proton energy at resonance. In the present determination of Q-value, the proton resonance energy was

Table 4. Transitions Used for Determining E_x Corresponding to the 2040 KeV Resonance in $^{29}Si(P, \gamma)^{30}P$ Reaction.

Transition Resonant State (r) → E_i	$E_x = E_\gamma + E_{recoil} + E_i$ (KeV)
$r \xrightarrow{11\%} 0$	7564.2±.18
$r \xrightarrow{3\%} 709$	7563.7±.21
$r \xrightarrow{15\%} 1455$	7563.8±.38
$r \xrightarrow{7\%} 3836$	7563.8±.66
$r \xrightarrow{6\%} 4736$	7564.0±.44
$r \xrightarrow{4\%} 4939$	7564.2±.49
$r \xrightarrow{16\%} 5506$	7564.3±.52
$r \xrightarrow{10\%} 5702$	7564.0±.46

Average E_x (KeV) = 7564.00±0.2

E_p (KeV) = 2039.8±0.5

$$E_x = \text{Q-value} + \frac{\text{mass of target nucleus}}{\text{mass of compound nucleus}} \times E_p$$

$$E_x = Q + \frac{29}{30}\ (2030.8)$$

Q-value $= E_x - 0.967 \times 2030.8$

$= 7564.0 - 1972.5$

Q-value = 5591.5±3 KeV

taken from the precise energy values for the proton resonances recently reported by Poirier et al. (55). The present Q-value is 0.5 KeV less than the value given in the 1964 mass table (60). Recent experimental determinations of the Q-value for the $^{29}Si(p,\gamma)^{30}P$ reaction are given in Table 5.

Table 5. Q-Value Determinations for the $^{29}Si(p,\gamma)^{30}P$ Reaction

Authors	Q-Value
Baart, Green, and Willmott (21)	5596 ± 12 KeV
Endt and Paris (18)	5570 ± 30 KeV
Harris and Hyder (1)	5597 ± 3 KeV
Present investigation	5591.5 ± 3.0 KeV

The branching ratios of the states in ^{30}P excited in this investigation are presented in Table 6. The results of previous measurements are also given for comparison. The results obtained for some of the levels are described below:

The 2539 KeV Level

This level is the second 3^+ state in ^{30}P. This level was excited in all the resonances studied in the work. The 2125 and 2410 KeV resonances decay strongly to this level. According to Sharpey-

Table 6. Branching Ratios of the Bound Levels in ^{30}P.

Initial State (KeV)	Final State (KeV)	E_γ (KeV)	Branching Ratios				
			Present work	Ref. 29	Ref. 19	Ref. 35,36	Ref. 30
2539	0	2539	97	≥85	95 ± 4	100	
	677	1862	3		< 5		
	709	1830					
	1455	1084			5 ± 4		
	1974	565			< 10		
2724	0	2724	100	≥80	100	100	
2839	0	2839	18 ± 2		22 ± 3	17 ± 3	22
	709	2130	46 ± 2		50 ± 4	49 ± 3	44
	1455	1384	37 ± 2		28 ± 4	34 ± 2	34
2939	0	2939	18 ± 2	19 ± 2	10 ± 6	17 ± 2	19
	677	2262	30 ± 2	37 ± 2	43 ± 6	32 ± 2	30
	709	2230	6 ± 2			9 ± 2	7
	1455	1484	46 ± 2	44 ± 2	47 ± 6	42 ± 2	44
3020	677	2343	100	≥95	100	100	
3836	0	3836			6 ± 3		
	677	3159			18 ± 6		
	709	3127					27
	1455	2381			16 ± 4		12
	2939	897	66 ± 6		60 ± 6	65	61
4183	709	3474	≥90	81 ± 3			
4736	0	4736			9 ± 5		
	677	4059			15 ± 5		
	709	4027					
	1455	3281			18 ± 5		
	2939	1797	63 ± 6		58 ± 6		
4939	677	4262	77 ± 6	≥70			
5207	0	5207	≥80				
5507	677	4830	≥85				≥80
5577	709	4868	≥60				
7502	2939	2763	≥60				≥80

Schafer et al. (35) this level decays 100 percent to the ground state, while, Vermette et al. (19) reported that there might be a 5 percent transition to the 1454 KeV level. In the present study it was found that this level decays 97 percent to the ground and 3 percent to the 709 KeV level. No transition to 1454 KeV level was observed as suggested by Vermette et al. (19).

The 2839 KeV Level

This level is populated at a few proton capture resonances. It was excited at E_p = 2125 and 2410 KeV. The branching ratios of 18 percent, 46 percent, and 37 percent to the ground state and the 709 and 1454 KeV levels are in agreement with the other recent measurements. Recently, Greene et al. (56) have pointed out an inconsistency with a previous spin assignment. They have suggested $J = 1^+$ in conflict with a previous $J = 3^+$ assignment (19, 29).

The 2939 KeV Level

This level was excited in all the resonances studied in this work. The 2234 and 2084 KeV resonances decay > 50 percent and > 80 percent to this level respectively. The branching ratios to the 677, 709, 1454 KeV levels and to the ground state are 30, 6, 46, and 18 percent, respectively, in general agreement with other recent measurements.

The 3836 KeV Level

This level is excited at 2040 and 2125 KeV resonances. The decays to 2939, 709, and 1454 KeV levels were observed in this investigation. Vermette et al. (19) reported a transition to 677 KeV level, but in the present work this level was found to decay to 709 KeV level rather than to 677 KeV level, in agreement with Din and Davis (30).

The 4736 KeV Level

This level decays 50% to the 2939 KeV level giving rise to a 1797 KeV γ-ray. Other transitions observed are to the 1454 KeV level and to the ground state. Bergstrom-Rohlin (28) have reported a strong 1800 KeV γ-ray which could not be fitted into the decay scheme of 1746 KeV resonance. The 4736 KeV level is perhaps excited at E_p = 1746 KeV which would explain the 1800 KeV γ-ray.

The 4938, 5206, 5508, 5577, and 5702 KeV Levels

Very little is known about these levels. These levels were excited at 2040 KeV resonance. The 4938 KeV level decays > 80% to 677 KeV level, 5206 KeV level goes to the ground state, 5508 KeV level decays > 85 percent to the 677 KeV level, 5577 KeV level

decays > 60 percent to the 709 KeV levek, and the 5702 KeV level decays > 60 percent to the 2939 KeV level.

4.4. Lifetime Measurements

The mean lifetimes of the excited states in ^{30}P, populated by the gamma decay of the E_p = 2040, 2125, and β410 KeV resonances in the $^{29}Si(p,\gamma)^{30}P$ reaction, were determined utilizing the Doppler-shift attenuation method (DSAM).

The γ-ray energies were measured with a 60-cm^3 Ge(Li) detector at θ_1 and θ_2 with respect to the proton beam. Relatively thick targets (10 - 12 KeV) were used to insure that the recoiling ^{30}P ions stopped completely in the target layer. The angles used were $\theta_1 = 0^\circ$ and $\theta_2 = 120^\circ$, except in one case when $\theta_2 = 90^\circ$ (2125 KeV resonance) was also used. From the measured energy shift $\Delta E_\gamma = E_\gamma(\theta_1) - E_\gamma(\theta_2)$, the attenuation factor

$$F(\tau) = \frac{\Delta E_\gamma}{E_{\gamma 0}\beta(0)(\cos\theta_1 - \cos\theta_2)}$$

was computed, where $E_{\gamma 0}$ is the γ-ray energy which results from emission by the nucleus at rest and $\beta(0) = \frac{v(0)}{c}$ is the initial recoil velocity of the ^{30}P ions. β(0) was obtained from the reaction kinematics. For the three resonances 2040, 2125, and 2410 KeV, β(0) = 0.0022, 0.0023, 0.0024 respectively. Whenever possible, the

weighted mean values of the Doppler shifts were determined from the shifts of the photopeaks and the double-escape-peaks in the spectra. To obtain the lifetime of an excited state, the measured $F(\tau)$ was compared with the value deduced from theoretical considerations, i.e.,

$$F(\tau) = \frac{1}{\tau} \int_0^\infty \frac{v(t)}{v(0)} \; e^{-\frac{1}{\tau}} \langle \cos \phi \rangle \, dt$$

where $\langle \cos \phi \rangle$ is the mean recoil scattering angle about the incident particle direction (6). Curves of $F(\tau)$ vs. τ were computed by numerical integration of the above equation using a computer program. $F(\tau)$ versus τ curves for the E_p = 2040, 2125, and 2410 KeV are shown in Figure 16. The details of the experimental set up and the technique of extracting lifetime information from the measured shifts (in γ-ray energy) are described in Section 2.4.

The resonance at E_p = 2040 KeV was found to be particularly useful for the lifetime work as is apparent from the decay scheme of this resonance shown in Figure 11. This resonance excites five levels in ^{30}P, which are either not populated at any other resonance or are excited at very few resonances. This resonance also decays to the other bound levels in ^{30}P which are also excited at a number of other resonances. In all, lifetimes of 10 levels were determined at this resonance. There are no previous lifetime measurements for

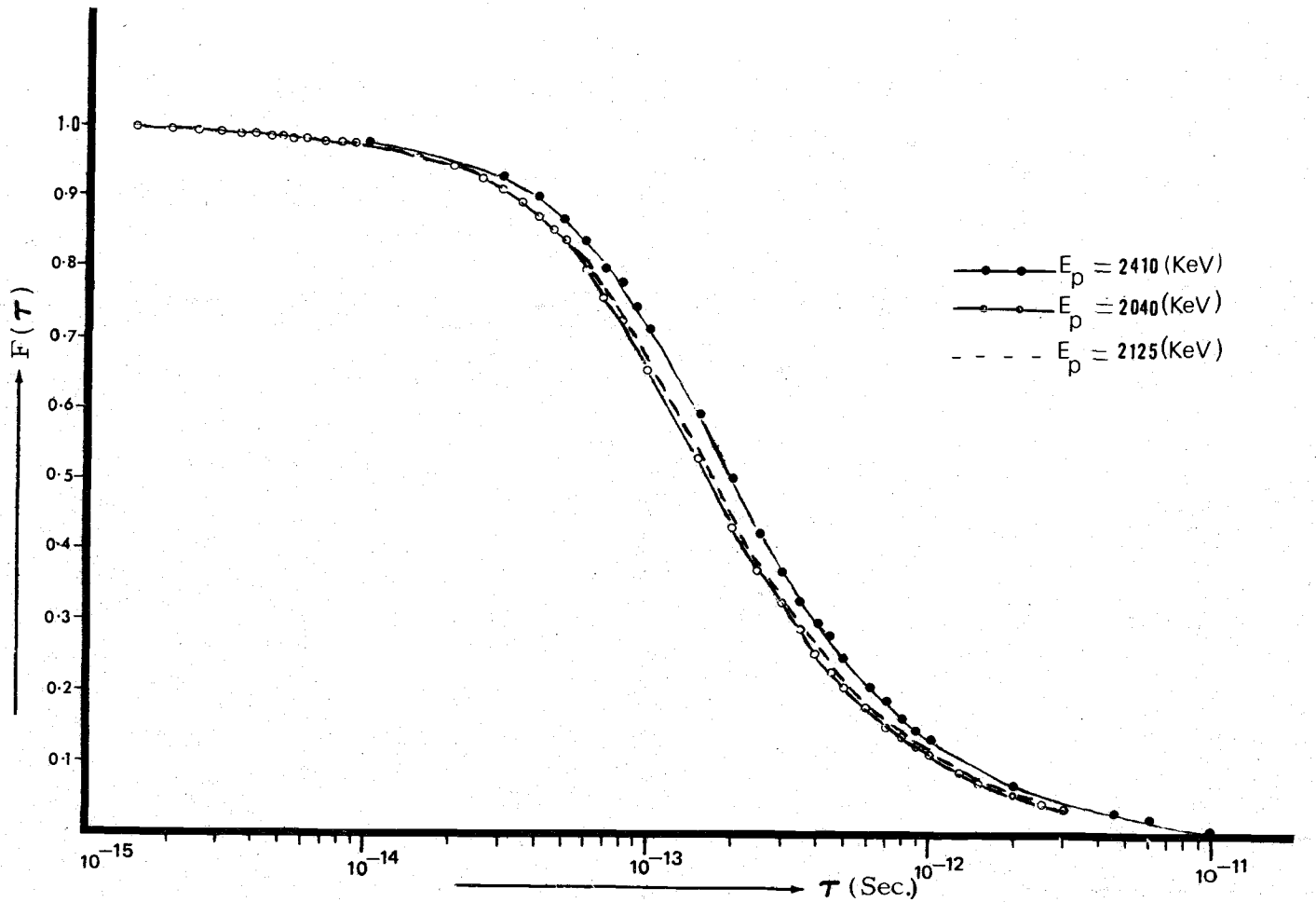

Figure 16. F(τ) vs. τ Curve

the levels at 4.74. 5.21, 5.51, 5.58, and 5.70-MeV excitation energies.

The resonance at E_p = 2125 KeV decays to the levels at 2.72, 2.54, 2.84, 2.94, 3.84, 4.18, 4.42, and 4.74 MeV in ^{30}P. The lifetimes of all of these levels, except the one at 2.94 MeV, were measured at this resonance. The lifetime of the 2.94 MeV level could not be determined because this level is also fed, besides the resonance state, by the 4.74 and 3.84 MeV levels having finite lifetimes. Moreover, there is no previous measurement on the lifetime of the 4.74 MeV level. The 2125 KeV resonance not only gave the lifetimes of the 4.42 and 2.84 MeV levels which were not excited at the 2040 KeV resonance, but also the lifetimes of the other levels which were also populated by the 2040 KeV resonances. This provided a useful check on the measurements at 2040 KeV resonance. The advantage of the 2125 KeV resonance is that it decays strongly to these levels compared with the resonance at 2040 KeV which populates many states.

The resonance at E_p = 2410 KeV decays strongly to the 2.54, 2.84, and 4343 KeV levels in ^{30}P. The level at 4343 KeV has not been reported in any (p, γ) experiment previously. Recently, Nolan et al. (35) have reported the lifetime of this level as 185 ± 15 fs. via the $^{27}Al(\alpha, n)^{30}P$ reaction and DSAM. The mean lifetime obtained in the present investigation was 220 ± 25 fs. The strong decay of this

resonance (40% of the total yield) to the 2.84 MeV level enabled accurate determination of the lifetime of this level as 2000 ± 800 fs.

The lifetime of the 2539 KeV level has been measured by a number of investigators. Using the reaction $^{29}Si(p,\gamma)^{30}P$, Harris and Hyder (29), Luukko et al. (34) and Graves and McDaniel (31) found a lifetime of 92 ± 21 fs., 53, and 260^{+90}_{-80} fs. respectively. Nolan et al. (35) determined a lifetime of 225 ± 20 fs. for this level via the reaction $^{27}Al(\alpha,n)^{30}P$. In all of these measurements DSAM was used for extracting the lifetime information. In the present experiment, lifetimes of 262 ± 10 fs. was obtained for this level. It was observed that the pulse shape of this γ-ray at $\theta = 0^{o}$ has two components (shown in Figure 17). The origin of these two components (62) lies in the slowing down mechanisms involved. The shifted component represents essentially the line shape that would be obtained if there were no nuclear stopping. The effect of the nuclear stopping mechanism, which is important at low recoil velocities, is to remove a fraction of the low-velocity recoiling ions from the tail of the pulse-shape distribution by suddenly stopping them: these ions subsequently decay to produce the stopped peak which is unshifted in energy. If the nuclear lifetime τ is small compared with the slowing down time α of the medium, then one would observe only the shifted component, if $\tau \gg \alpha$, then only the shifted component will be seen and if $\tau \approx \alpha$, then the pulse-shape will have two components. For a more precise

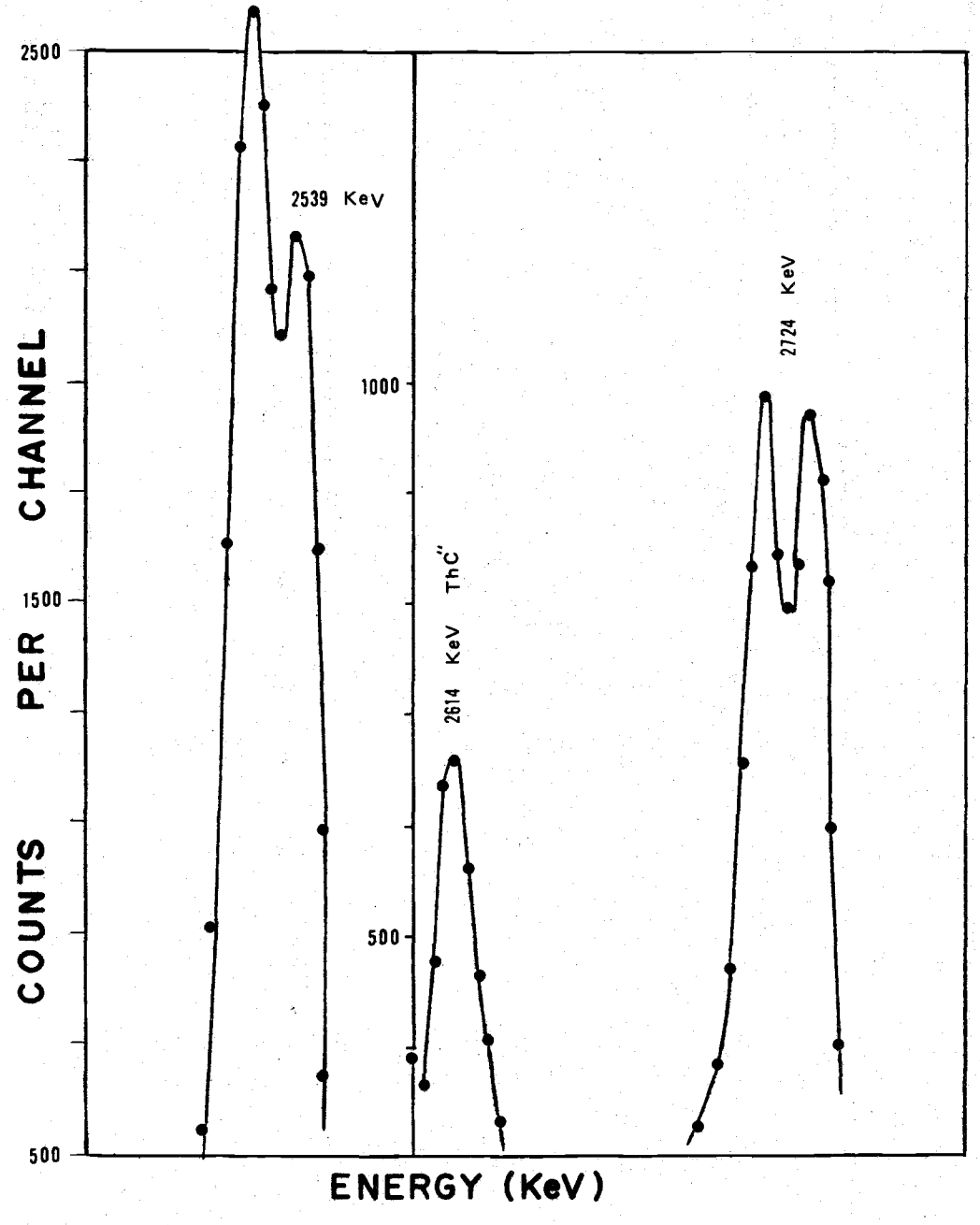

Fig.17 Line Shapes of 2539, 2614, and 2724 KeV Lines at $\theta = 0^{\circ}$ and $E_p = 2125$ KeV.

analysis, one should fit the experimental spectrum with a calculated line shape to determine the lifetime. However, considering the uncertainty in the energy-loss parameters (as large as 15%), the centroid analysis should give reasonably satisfactory results. This method was used in the analysis of Doppler shifts of the 2538, 2724, and 2370 KeV γ-rays to obtain lifetime information of the 2539, 2724, and the 4343 KeV levels. There is only one previous measurement on the lifetime of 4343 KeV level (35). The lifetime found in this work is in agreement with that measurement. The lifetime of the 2724 KeV level is in agreement with Graves and McDaniels (31), but in disagreement with Harris and Hyder (29). Table 7 shows the DSA results obtained in this work. A summary of the lifetime measurements, present and previous, is presented in Table 8. Experimental results for the γ-ray transition strengths in ^{30}P are compared, in Table 9, with the available theoretical predictions. The agreement between the observed and the intermediate-coupling model (46) predictions for the E2 transitions appears to be good, but the predicted M1 transition rates seem to depart rather markedly from the experimentally observed rates.

Table 7. Results of DSA Measurements.

E_x (KeV)	E_γ (KeV)	E_p (KeV)	$F(\tau)$	τ_m (10^{-15} sec)
2539	2539	2040	0.36 ± 0.06	260^{+70}_{-50}
		2125	0.37 ± 0.02	262 ± 10
2724	2724	2125	0.47 ± 0.04	190 ± 25
2839	2130	2410	0.07 ± 0.02	2200^{+800}_{-700}
3020	2343	2040	≥ 0.94	≤ 21
3836	897	2125	0.84 ± 0.03	52 ± 8
4183	3474	2040	≥ 0.95	≤ 17
		2125	≥ 0.92	≤ 28
4343	2369	2410	0.47 ± 0.04	220 ± 25
4422	4422	2125	0.80 ± 0.03	62 ± 8
4736	1797	2040	0.69 ± 0.07	90^{+22}_{-20}
		2125	0.70 ± 0.04	90 ± 14
4939	4262	2040	≥ 0.96	≤ 15
5207	5207	2040	0.91 ± 0.04	30 ± 12
5507	4830	2040	≥ 0.97	≤ 10
5577	4868	2040	≥ 0.94	≤ 21
5702	2763	2040	0.94 ± 0.02	21 ± 7

Table 8. Summary of the Lifetime Information on ^{30}P.

Level Energy (KeV)	T_m (fs.)							
	Present work	Ref. 31	Ref. 29	Ref. 35,36	Ref. 34	Ref. 33	Ref. 38	Ref. 32
2539	262 ± 10	260^{+90}_{-80}	92 ± 21	225 ± 20	53, 80 ± 25			
2724	190 ± 25	160 ± 20	84 ± 17 126 ± 27	175 ± 35		148 ± 22		
2839	2200 ± 800	750^{+250}_{-170}		1200 ± 200	<160, <230		3000^{+2000}_{-1000}	
3020	<21	<10		<30	<8, <12	<29		<15
3836	52 ± 8	44 ± 7		32^{+15}_{-12}				
4183	<20	< 24		<20		<20		<15
4343	220 ± 25			185 ± 15				
4422	62 ± 8	58 ± 6	64 ± 8		13, 19 ± 8	40 ± 7		
4736	90 ± 14							
4939	<15	< 25	47 ± 20					
5207	30 ± 15							
5507	<10							
5577	<21							
5702	<21							

Table 9. Comparison of Measured γ-ray Transition Strengths in ^{30}P with Available Theoretical Predictions.

Transition $E_i \rightarrow E_f$ (KeV)	$J_i^\pi \rightarrow J_f^\pi$	δ Ref. 19	$\lvert M(E2)\rvert^2$ W.u.			$\lvert M(M1)\rvert^2$ m W.u.		
			Measured	Shell Model	I.C. Model	Measured	Shell Model	I.C. Model
2539 → 0	$3^+ \rightarrow 1^+$	0	5.03	0.0	5.4			
2539 → 709	$3^+ \rightarrow 1^+$	0	0.80	1.3	0.2			
2724 → 0	$2^+ \rightarrow 1^+$	3.0	4.54	0.0	4.5	0.80	0.0	0.02
2839 → 0	$(3)^+ \rightarrow 1^+$	a	0.06		1.5			
2839 → 709	$(3)^+ \rightarrow 1^+$	a	0.69		0.8			
3020 → 677	$1^+ \rightarrow 0^+$	0				$\geq$ 54.1		0.64

a) mixing ratios not known; electromagnetic strengths calculated assuming pure multipolarities.

V. SUMMARY AND CONCLUSIONS

The $^{29}Si(p, \gamma)^{30}P$ reaction has been used to obtain more information on the levels in ^{30}P between 2.0 and 5.7 excitation energy. The decay schemes and branching ratios of the 2040, 2084, 2125, 2234, and 2410 KeV resonances were investigated using a large volume Ge(Li) detector.

Accurate measurements of the γ-ray energies made it possible to determine more precise values of the energies of the ^{30}P excited states up to 5.70 MeV excitation energy with errors ranging from 0.5 to 2 KeV.

A new Q-value of 5591.5 ± 3 KeV was obtained from nine γ-ray cascade transitions in the γ-decay of the 2040 KeV resonance.

The decay schemes for the resonances studied in this investigation have provided new information about the bound levels in ^{30}P. The levels at 5.70, 5.58, 5.51, 5.21, 4.94, 4.74, and 3.84 MeV were excited by the deexcitation of the 2040 KeV resonance. These levels are either not populated at any other (p, γ) resonance or are excited only at a few resonances. The level at 5.58 MeV excitation energy has not previously been reported. A level at 4343 KeV excitation energy in ^{30}P was excited by the γ-decay of 2410 KeV resonance. This level has not been studied at any other (p, γ) resonance.

The information about the spins and parities of these levels is

lacking. This information could be obtained by measuring angular distributions at these resonances.

Doppler-shift attenuation method has been used to obtain life-time information about a number of levels populated in the decay of 2040, 2125, and 2410 KeV resonances. The measured lifetimes (in fs.) are as follows:

2539 KeV level (262 ± 10), 2724 KeV level (190 ± 25), 2839 KeV level (2200 ± 800), 3020 KeV level (< 21), 3836 KeV level (52 ± 8), 4183 KeV (< 20), 4343 KeV level (220 ± 25), 4422 KeV level (62 ± 8), 4736 KeV level (90 ± 14), 4939 KeV level (< 15), 5206 KeV level (30 ± 15), 5507 KeV level (< 10), 5577 KeV level (< 21), and 5702 KeV level (< 21).

There are no previous measurements on the lifetimes of 4736, 5206, 5506, 5577, and 5702 KeV levels.

A fairly comprehensive picture of the electromagnetic decay properties of ^{30}P for levels in the region of excitation energy $0 \leq E_x \leq 5.70$ MeV can be constructed by using the results of the present study together with the results of previous measurements presented in Tables 1 to 9. This information can then be used to test the validity of a given model designed to explain the structure of ^{30}P nucleus.

BIBLIOGRAPHY

1. Harris, G.I., and Hyder, A.K., Jr., Properties of ^{30}P levels from the ^{29}Si(p, γ)^{30}P reaction. Phys. Rev., 157, 958 (1967).

2. Endt, P.M., and Van der Leun, C., Energy levels of Z = 11-21 nuclei. Nucl. Phys. A105, 1 (1967).

3. Dolan, K.W. et al. Calibration of high-energy gamma rays. Bull. Am. Phys. Soc. 12, 914 (1967).

4. King, G.D. et al. The energy of the ^{40}K gamma rays and its use as a calibration standard. Nuclr. Instr. & Methods 52, 349 (1967).

5. Murray, G. et al. The precision determination of some gamma ray energies using a beta spectrometer. Nucl. Phys. 63, 353 (1965).

6. Blaugrund, A.E. Notes on Doppler shift lifetime measurements. Nucl. Phys. 88, 501 (1966).

7. Lindhard, J. et al. Range concepts and heavy ion ranges. Kgl. Denske Videnskab Selskal, Mat. Fys. Medd. 33, #14 (1963).

8. Devons, S. et al. Measurement of γ-transition lifetimes by recoil methods. Proc. Phys. Soc. A68, 18 (1955).

9. Litherland, A.E. et al. Lifetimes of the low-lying levels of ^{18}O and ^{18}F. Nucl. Phys. 44, 220 (1963).

10. Warburton, E.K. et al. Lifetimes of the ^{10}Be 3.37-MeV level. Phys. Rev. 129, 2180 (1963).

11. Currie, W.M. et al. Experimental problems in the Doppler shift attenuation method. Nucl. Phys. A135, 325 (1969).

12. Broud, C. et al. Dependence of the Doppler shift lifetime method on the slowing environment. Phys. Lett. 39B, 185 (1972).

13. Caraca, J.M.G. et al. Transition strengths in ^{37}Ar and ^{35}Cl. Nucl. Phys. A176, 273 (1971).

14. Hartmann, R., and Graw, H. Doppler shift attenuation measurements in ^{42}Ca. Nucl. Phys. A164, 209 (1971).

15. Ormrod, J.H., and Duckworth, H.E. Stopping cross sections in carbon for low-energy atoms with $Z \leq 12$. Can. J. Phys. 41, 1224 (1963).

16. Fastrup, B. et al. Stopping cross sections in Carbon of 0.1 - 1.0 MeV atoms with $6 \leq Z_1 \leq 20$. Mat. Fys. Medd. Dan Vid. Selsk 35, #10 (1965).

17. Kramer, R. Thesis, Freiburg 1970, Unpublished. (Details in ref. 14).

18. Endt, P.M., and Paris, C.H. Nuclear levels in ^{30}P, ^{33}S, and ^{35}S. Phys. Rev. 110, 89 (1958).

19. Vermette, C.W. et al. A study of ^{30}P levels below 5 MeV. Nucl. Phys. A111, 39 (1968).

20. Van der Leun, C. and Endt, P.M. Investigation of four resonances in the reaction $^{29}Si(p, \gamma)^{30}P$. Phys. Rev. 110, 96 (1958).

21. Baart, E.E. et al. An investigation of the $^{29}Si(p, \gamma)^{30}P$ reaction. Proc. Phys. Soc. (London) 79, 237 (1962).

22. Broud, C. et al. Low-lying levels of ^{30}P. Phys. Rev. 101, 1052 (1956).

23. Moor, R.A. Thesis, University of Kansas, 1963 (unpublished).

24. Val'ter, A.K. et al. Investigation of the γ-rays associated with the 1308 KeV resonance in $^{29}Si(p, \gamma)$ reaction. Izv. Akad. Nauk. SSSR Ser Fiz 27, 242 (1963).

25. Ejiri, H. et al. Gamma rays from the reaction $^{29}Si(p, \gamma)^{30}P$. Nucl. Phys. 51, 470 (1964).

26. Val'ter, A.K. et al. Quantum characteristics of the 6847 MeV level of ^{30}P observed in the reaction $^{29}Si(p, \gamma)^{30}P$. Soviet Phys. JETP 14, 1035 (1962).

27. Phelps, P.A. et al. Some energy levels in ^{30}P observed in radiative capture by ^{29}Si of protons with energy from 1420 to 2160 KeV. Phys. Rev. 138B, 1088 (1965).

28. Bergstrom-Rohlin, S. Investigation of the $^{29}Si(p, \gamma)^{30}P$ reaction at proton energies 1460 to 1860 KeV. Arkiv Fysik 35, 349 (1968).

29. Harris, G.I. et al. Properties of ^{30}P levels from the reaction $^{29}Si(p, \gamma)^{30}P$. Phys. Rev. 187, 1413 (1969).

30. Din, G.U., and Davis, J.R. A study of the resonances in the $^{29}Si(p, \gamma)^{30}P$ reaction. Aust. J. Phys. 24, 497 (1971).

31. Graves, R., and McDaniels, D.K. Lifetimes in ^{30}P by the $^{29}Si(p, \gamma)^{30}P$ reaction. Bull. Am. Soc. 14, 1173 (1969).

32. Lachain, A., and Hird, B. Some Doppler shift lifetimes in ^{30}P. Can. J. Phys. 48, 2337 (1970).

33. Bini, M. et al. Lifetimes of some levels in ^{30}P Nuovo Cim A4, 45 (1971).

34. Luuko, A. et al. Lifetimes of energy levels in ^{30}P. Physica Scripta Vol. 15, 63 (1972).

35. Sharpey-Schafer, et al. Lifetimes and decays of energy levels in ^{30}Si and ^{30}P. Nucl. Phys. A167, 602 (1971).

36. Nolan, P. et al. Lifetime measurements for levels in ^{30}P between 3.7 and 4.7 MeV excitation energy. J. Phys. A: General Phys. Vol 5, 454 (1972).

37. Kennedy, E.F. et al. Lifetimes of the two levels in ^{30}P. Phys. Rev. 158, 897 (1967).

38. Pixley, R.E., and Poletti, A.R. Lifetimes of low-lying states in ^{30}P by DSAM. Bull. Am. Phys. Soc. 14, 125 (1969).

39. Glaudemans, P.W.M. et al. Shell model calculations in the $2S_{1/2}$ and $1d_{3/2}$ shell. Nucl. Phys. 56, 529 (1964).

40. Hanson, S.H. et al. Recoil distance lifetime measurements for states in ^{30}P. Phys. Rev. C3, 191 (1971).

41. Picard, J., and de Pinho, A.G. Theoretical calculations for ^{30}P. Nuovo Cim 41B, 239 (1966).

42. Wasielewski, P. and Malik, F. B. Approach of the unified model with coriolis coupling to ^{22}Na, ^{26}Al, and ^{30}P. Nucl. Phys. A160, 113 (1971).

43. Ascuitto, R. J. et al. Symmetric core collective model for odd-odd nuclei with applications in the 2s-1d shell. Phys. Rev. 176, 175 (1968).

44. Thankappan, V. K. and Pandya, S. P. Collective vibrations in ^{31}P. Nucl. Phys. 19, 303 (1960).

45. Bouten, M. C. et al. Intermediate coupling in the nuclear ds-shell. Nucl. Phys. A97, 113 (1967).

46. Singh, B. P. et al. Nuclear structure of ^{30}P and ^{34}Cl in a unified model. Phys. Rev. C5, 1613 (1972).

47. Glaudemans, P. W. M. et al. Shell model calculations on energy levels in the $2S_{1/2}$-$1d_{3/2}$. Nucl. Phys. A56, 529 (1964).

48. Wildenthal, B. H. et al. Structure of nuclei with mass A = 30-35 as calculated in the shell model. Phys. Rev. C4, 1708 (1971).

49. Glaudemans, P. W. M. et al. Shell model calculations of e.m. transition rates and multipole moments in A = 30 - 34. Annals of Phys. 63, 134 (1971).

50. Marion, J. B. γ-ray calibration energies. Nuclear Data A4, 301 (1968).

51. Ophel, T. R., and Osgood, D. R. The 992 KeV resonance of the ^{27}Al(p, γ) reaction. Proc. Phys. Soc. 85, 1093 (1965).

52. Endt, P. M., and Van der Leun, C. Energy levels of Z = 11 - 21 nuclei. Nucl. Phys. A105, 1 (1967).

53. L'vov, A. N. et al. Levels of ^{30}P. Bull. Acad. Sci. USSR Phys. Ser. 30, 447 (1966).

54. Storizhko, V. E. and Popov, A. I. Levels of ^{30}P evinced in the ^{29}Si(p, p)^{29}Si reaction. Bull. Acad. Sci. USSR Phys. Ser. 28, 1054 (1965).

55. Poirier, C.P., et al. Elastic and inelastic proton resonances on ^{29}Si. Phys. Rev. C1., 1984 (1970).

56. Greene, M.W. et al. Core excitation in ^{30}P. Phys. Lett. 32B, 680 (1970).

57. Kostin, V.Y., et al. Levels in ^{30}P at 7.5 to 8.5 MeV. Ukr. Fiz. Zhurnal, vol. 17, 199 (1972).

58. Murray, G. et al. The precision determination of some gamma ray energies using a beta-spectrometer. Nucl. Phys. 63, 353 (1965).

59. Gunnink, R. et al. ^{56}Co. gamma ray energies. Nucl. Instr. and Methods 65, 26 (1968).

60. Mattauch, J.H.E. et al. 1964 Atomic mass table. Nucl. Phys. 67, 32 (1965).